ACCEPTED FOR PUBLICATION IN THE ASTROPHYSICAL JOURNAL
Preprint typeset using LaTeX style emulateapj v. 14/09/00

A BRIDGE FROM OPTICAL TO INFRARED GALAXIES: EXPLAINING LOCAL PROPERTIES, PREDICTING GALAXY COUNTS AND THE COSMIC BACKGROUND RADIATION

TOMONORI TOTANI[1, 2, 3] AND TSUTOMU T. TAKEUCHI[4, 5, 6]
Accepted for Publication in the Astrophysical Journal

ABSTRACT

We give an explanation for the origin of various properties observed in local infrared galaxies, and make predictions for galaxy counts and cosmic background radiation (CBR), by a new model extended from that for optical/near-infrared galaxies. Important new characteristics of this study are that (1) mass scale dependence of dust extinction is introduced based on the size-luminosity relation of optical galaxies, and that (2) the big grain dust temperature $T_{\rm dust}$ is calculated based on a physical consideration for energy balance, rather than using the empirical relation between $T_{\rm dust}$ and total infrared luminosity $L_{\rm IR}$ found in local galaxies, which has been employed in most of previous works. Consequently, the local properties of infrared galaxies, i.e., optical/infrared luminosity ratios, $L_{\rm IR}$-$T_{\rm dust}$ correlation, and infrared luminosity function are outputs predicted by the model, while these have been inputs in a number of previous models. Our model indeed reproduces these local properties reasonably well. Then we make predictions for faint infrared counts (in 15, 60, 90, 170, 450, and 850 μm) and CBR by this model. We found considerably different results from most of previous works based on the empirical $L_{\rm IR}$-$T_{\rm dust}$ relation; especially, it is shown that the dust temperature of starbursting primordial elliptical galaxies is expected to be very high (40–80K), as often seen in starburst galaxies or ultra luminous infrared galaxies in the local and high-z universe. This indicates that intense starbursts of forming elliptical galaxies should have occurred at $z \sim 2$–3, in contrast to the previous results that significant starbursts beyond $z \sim 1$ tend to overproduce the far-infrared (FIR) CBR detected by *COBE*/FIRAS. On the other hand, our model predicts that the mid-infrared (MIR) flux from warm/nonequilibrium dust is relatively weak in such galaxies making FIR CBR, and this effect reconciles the *prima facie* conflict between the upper limit on MIR CBR from TeV gamma-ray observations and the *COBE* detections of FIR CBR. The intergalactic optical depth of TeV gamma-rays based on our model is also presented.

Subject headings: cosmology: observations — galaxies: evolution — galaxies: formation

1. INTRODUCTION

To understand when and how stars and galaxies formed in the universe is one of the most fundamental issues in modern astronomy. The energy emitted from stars as a result of nuclear fusion is radiated in two modes: direct stellar emission ranging from optical to near-infrared (NIR) wavelengths, and emission in mid- and far-infrared (MIR and FIR) wavelengths from dust particles heated by stellar radiation field.[7] Faint galaxy counts and the cosmic background radiation (CBR), as well as the properties of galaxies in the local universe, give us important clues to understand galaxy formation.

In optical/NIR wavelengths, the sensitivity of existing telescopes now reaches a depth sufficient to resolve more than 80–90% of CBR from galaxies (Totani et al. 2001a), thanks to very deep optical surveys such as the Hubble Deep Fields (HDFs: Williams et al. 1996; Williams et al. 2000) and the NIR surveys such as the Subaru Deep Field (SDF: Maihara et al. 2001). There are a number of theoretical models in various approaches to be compared with these data, and in fact these data can be reasonably explained in the framework of the Big-Bang cosmology and structure formation induced by the cold dark matter (CDM). In contrast, infrared observations have not yet reached such depth and star formation activity hidden by dust extinction is still poorly known, despite the dramatic progress of observations achieved by satellites such as *IRAS* (e.g., Soifer et al. 1987 and references therein) and *ISO* (e.g. Puget et al. 1999; Oliver et al. 2000; Okuda 2000; for a review, see e.g., Genzel & Cesarsky 2000). The SCUBA of JCMT (Holland et al. 1999) has opened a new window of submillimeter wavelengths to probe the dusty galaxies at high-z, and it seems that a considerable part of CBR from submm galaxies has been resolved (e.g., Smail, Ivison, & Blain 1997; Hughes et al. 1998; Blain et al. 1999; Blain et al. 2000; Eales et al. 1999, 2000; and Barger et al. 1998, 1999). However, insufficient angular resolution does not allow us to identify most of these objects in other wavelengths. Forthcoming projects such as *SIRTF*, *ASTRO-F*, SOFIA, *Herschel Space Observatory*, *NGST*, and ALMA would bring about revolutionary progress from this situation. Comparison of these data with theoretical models of infrared galaxies will be the key to understand the "dark side" of galaxy formation in the next decade of extragalactic astronomy.

Theoretical modeling of galaxy formation and evolution has a long history. In optical/NIR wavelengths, most theoretical

[1] Princeton University Observatory, Princeton, NJ 08544-1001, USA
e-mail: ttotani@princeton.edu
[2] Theory Division, National Astronomical Observatory, Mitaka, Tokyo 181-8588, Japan
[3] Postdoctoral Fellow of the Japan Society for the Promotion of Science (JSPS) for Research Abroad
[4] Optical and Infrared Astronomy Division, National Astronomical Observatory, Mitaka, Tokyo 181-8588, Japan
[5] Institute of Astronomy, Faculty of Science, the University of Tokyo, Mitaka, Tokyo 181-0015, Japan
[6] Research Fellow of the Japan Society for the Promotion of Science (JSPS).
[7] In this paper, the term 'infrared' refers to the emission from dust particles in the MIR and FIR including submillimeter, but excluding direct stellar emission in the NIR.

modelings can be roughly divided into two categories: the so-called "backwards" approach and "*ab initio*" approach. In the former approach (Tinsley 1980; Yoshii & Takahara 1988; Fukugita et al. 1990; Rocca-Volmerange & Guiderdoni 1990; Yoshii & Peterson 1991, 1995; Pozzetti et al. 1996, 1998; Jimenez & Kashlinsky 1999; Totani & Yoshii 2000), the luminosity function of local galaxies is used as an input to normalize the number density of galaxies. The local properties of galaxies such as multi-band colors and chemical properties are also used to construct a reasonable model of star formation history and luminosity evolution of galaxies based on the stellar population synthesis method. The evolution is then probed backwards into the past to predict observables such as galaxy counts and redshift distributions. The formation epoch and merging history of galaxies cannot be predicted in this framework, and hence they are introduced as phenomenological parameters that can be inferred from comparison with observational data. In the latter approach (Kauffmann et al. 1993; Cole et al. 1994, 2000; Somerville & Primack 1999; Nagashima et al. 2001), on the other hand, the formation epoch and merging history of galaxies are predicted by the standard theory of structure formation in the CDM universe. In these models the local properties such as luminosity function are outputs of the model which should be compared with observations. However, although the formation and evolution of dark matter halos are rather well understood and can be properly predicted, our knowledge about baryonic processes such as star formation, supernova feedback, or galaxy merging is still very poor, and a number of phenomenological parameters must be incorporated, making the comparison of a model and observed data rather complicated.

Both of these two approaches have been used also to make predictions of infrared galaxy counts and infrared CBR (see Franceschini et al. 1994 for the former, Guiderdoni et al. 1998 and Devriendt & Guiderdoni 2000 for the latter, and Tan, Silk, & Balland 1999 for a somewhat hybrid approach between the two). However, because of our poor knowledge and understanding of dust formation and emission, there are considerable difficulties in theoretically predicting infrared luminosity, spectral energy distribution (SED), and their evolution of dust emission, compared with the optical/NIR modeling based on the stellar population synthesis method. This is the motivation of another "empirical" approach[8] in the MIR and FIR wavelengths. In this kind of approach, the infrared luminosity evolution is introduced by some phenomenological functional forms and constraints on luminosity evolution is derived from comparison with observed data (Beichman & Helou 1991; Oliver, Rowan-Robinson & Saunders 1992; Blain & Longair 1993, 1996; Pearson & Rowan-Robinson 1996; Malkan & Stecker 1998, 2001; Takeuchi et al. 1999, 2001a, 2001b; Roche & Eales 1999; Gispert, Lagache, & Puget 2000; Wang & Biermann 2000; Xu et al. 2001; Franceschini et al. 2001).

There is yet another approach so-called "cosmic chemical evolution", in which the universe is treated as a uniform medium and the mean gas consumption by stars in the whole universe is considered (Pei & Fall 1995; Fall, Charlot, & Pei 1996; Pei, Fall, & Hauser 1999; Sadat, Guiderdoni, & Silk 2001). The cosmic star formation history is determined by the redshift evolution of the cosmic mass density of neutral gas and the cosmic mean metallicity, which is inferred from quasar absorption line systems. Although this is a simple and beautiful approach to predict CBR (but not galaxy counts), several problems exist in this kind of approach, which could be serious especially in modeling infrared radiation from dust. First, quasar absorption systems are inevitably biased to gas-rich systems, i.e., systems in which star formation has been relatively inefficient, and hence their mean metallicity does not necessarily represent the mean of the whole universe. For example, if an elliptical galaxy has formed at $z \sim 4$, this galaxy has been already in passive evolution phase at $z \sim 2$. Then it can never be observed as a quasar absorption system because of complete exhaustion of interstellar gas, although significant stars and metals have been produced. Galaxies in dusty starburst phase may not be traced by absorption line systems, either, because background quasars may be completely extincted and cannot be observed. Therefore, the metallicity and star formation activity observed in absorption line systems must be an underestimate of the true mean in the universe. Furthermore, extinction by interstellar dust and reradiation in infrared bands are very sensitively dependent on dust opacity and its geometrical distribution within a galaxy, but this important information is completely missed.

In this paper we construct a model of infrared galaxy counts and CBR based on the backwards approach for luminosity evolution of galaxies, by extending the model for optical/NIR galaxy counts (Totani & Yoshii 2000, hereafter TY00) to include dust emission component in infrared bands. After the work by Franceschini et al. (1994, F94 hereafter), only a limited number of models have been published based on this approach covering FIR bands, while there has been a dramatic increase of quality and quantity of observational data in the local universe as well as for faint/high-z galaxies. Although the backwards approach has a disadvantage that formation epoch and merger history must be treated phenomenologically, it has an advantage that the number of model parameters is much fewer, and connection of the model galaxies to the local galaxy populations is clearer, than the *ab initio* approach. Another reason for the relatively low activity of work in this direction is the difficulty of constructing realistic evolutionary models that can consistently describe both the optical and infrared data at the local universe as well as high-z, as argued by Franceschini et al. (2001). This is indeed what motivated more empirical studies confined to the infrared bands.

The aim of this paper is to explain the bulk of optical and infrared data consistently by realistic evolutionary models of known and relatively normal galaxy populations at the local universe, without introducing hypothetical populations or parametric description of luminosity evolution. An important improvement of our model from the F94 model is that mass scale dependence is introduced for dust extinction and reradiation, based on the size-luminosity relation of galaxies observed in the optical bands. In the F94 model, there was no physical difference in model galaxies of a given type with different masses; massive galaxies were simply a scaled-up version of smaller objects. We will show that this point is essential to understand various local properties of infrared galaxies.

Another important characteristic of this work is modeling of the infrared SED evolution. In most of the previous infrared models, including *ab initio* and empirical approaches, the dust SED is empirically modeled in such a way that the dust SED is a one-parameter family specified by the total infrared luminosity of galaxies. The relation between the dust SED and luminosity,

[8] In several publications this approach is also referred to a "backwards" approach, but here we discriminate between the "backwards" approach mentioned earlier and the "empirical" approach.

which is observed in local infrared galaxies, is characterized by a gradual increase of characteristic dust temperature $T_{\rm dust}$ with infrared luminosity $L_{\rm IR}$ and is often expressed simply as a linear relation between $T_{\rm dust}$ and $\log L_{\rm IR}$ (e.g. Smith et al. 1987; Soifer & Neugebauer 1991). However in this paper, we argue that this relation is not physically warranted for high-z galaxies. In a physical sense, the luminosity is *extensive*, i.e., a quantity which is dependent upon the amount of substance present in the system. On the other hand, the dust temperature is *intensive*, which is a specific characteristic of the system and is independent of the amount of material concerned. Therefore these two must not be related by only one sigle relation. At least there should be another extensive quantity such as the total mass of dust in a galaxy $M_{\rm dust}$. In the empirical $L_{\rm IR}$-$T_{\rm dust}$ relation, the extensive scale of an object is completely missed. The empirical $L_{\rm IR}$-$T_{\rm dust}$ relation of local infrared galaxies should be considered as a projection of the plane between $L_{\rm IR}$, $T_{\rm dust}$, and $M_{\rm dust}$. Here we will construct a model on physical basis to describe the infrared luminosity as a two-parameter family of $M_{\rm dust}$ and $T_{\rm dust}$. The dust temperature is physically calculated, without using the empirical $L_{\rm IR}$-$T_{\rm dust}$ relation. In addition to the thermal emission from big grain dust, the warm/nonequilibrium components of dust emission from small grain dusts and PAH features are also added to the model SED to be consistent with the observed infrared SED of galaxies.

It is important to check that the model can successfully reproduce the local properties of infrared galaxies, before predicting the high-z quantities such as counts and CBR, since in our model all the inputs are the optical/NIR properties of local galaxies, and those in infrared bands are outputs predicted by the model. We will compare the model prediction with the observed properties of local infrared galaxies, such as the correlation between optical and infrared luminosity, the $L_{\rm IR}$-$T_{\rm dust}$ relation, and infrared luminosity function. Indeed, we will show that our model gives a reasonable explanation for these relations as well as the scatter along the mean relation. Recently Granato et al. (2000) have presented a very sophisticated semi-analytic model of infrared galaxy formation to calculate various properties of local infrared galaxies, although predictions for high-z galaxies have not been made yet. They have also found that most of the observed properties can be reproduced in their model framework. However, a large number of parameters have been introduced to treat various physical processes, and the origin of the observed properties of local infrared galaxies has not been clearly discussed. Here we try to shed light on the underlying physics of these properties by a model with a much fewer number of adjustable parameters.

Then we will make predictions of infrared galaxy counts and CBR by our backwards evolution model. We found that the empirical $L_{\rm IR}$-$T_{\rm dust}$ relation breaks down at high-z, especially in the intense starbursts expected at the formation of elliptical galaxies. The dust temperature should be much higher (40–80K) than predicted by mere extrapolation of the empirical $L_{\rm IR}$-$T_{\rm dust}$ relation. We will discuss the implications of our results for the star formation history of the universe, especially the formation epoch of elliptical galaxies. Our result also has an interesting implication for the *prima facie* conflict (Stecker 2000) between the upper limit on MIR CBR from TeV gamma-ray observations and the FIR CBR detections by the *COBE* satellite. The calculation of intergalactic optical depth of TeV gamma-rays based on our model will also be presented.

The paper will be organized as follows. The model of galaxy evolution in the optical bands, on which the infrared modeling is based, will be summarized in §2. Then the extension of the optical/NIR model to include the dust emission is described in detail in §3. Our model predicts local properties of infrared galaxies, and they are compared with the observations in §4. The predictions of faint infrared counts and CBR will be presented to be compared with observed data, in §5. Implications and discussions on our results are given for several topics in §6, and finally we summarize and conclude this paper in §7. Unless otherwise stated, we will adopt a cosmological model with $h = H_0/(100{\rm km/s/Mpc}) = 0.7$, $\Omega_0 = 0.2$, $\Omega_\Lambda = 0.8$.

2. MODEL OF OPTICAL/NIR GALAXIES

We use the same model as that used in TY00, which is in overall agreement with the optical counts and photometric redshift distributions in HDF (TY00), and K-band counts, colors, and size distributions in the SDF (Totani et al. 2001c). The detail of the model is given in TY00 and here we summarize important properties of the model. Although active galactic nuclei (AGNs) may have some contributions to infrared galaxy counts and CBR, most of previous studies indicate that they are not the dominant population in counts or CBR (e.g. Rigopoulou et al. 2000; Barger et al. 2001). Therefore we will consider only normal galaxies without AGNs. Galaxies are classified into five morphological types of E/S0, Sab, Sbc, Scd, and Sdm, and their evolution of luminosity and spectral energy distributions (SEDs) is described by a standard galaxy evolution model in which their star formation history is determined to reproduce the present-day colors and chemical properties of galaxies (Arimoto & Yoshii 1987; Arimoto, Yoshii, & Takahara 1992). These models include chemical evolution giving gas fraction $f_{\rm gas}$ and metallicity Z as a function of time and morphological type. We assume that the original dust-free SED of galaxies and its evolution do not depend on the galaxy luminosity (or mass). Their SED evolutions are shown in Fig. 1 of TY00. The number density and morphological type mix are determined by the type-dependent present-day B-band luminosity function, and here we adopt that of SSRS2 survey (Marzke et al. 1998). Therefore, galaxies in our model are identified by morphological type and present-day B luminosity. All galaxies are assumed, for simplicity, to be formed at a single redshift, z_F. We will adopt the formation redshift within a range of $z_F = 2$–5 to see the sensitivity of our predictions on this parameter.

A unique characteristic of the TY00 model is that the size and luminosity profile of galaxies are modeled and used to calculate the detection completeness of high-z galaxies in a realistic way based on the formulation developed by Yoshii (1993). Selection effects are very important in optical bands because galaxies are detected as extended sources and galaxy images are significantly affected by observational seeing and the cosmological dimming of surface brightness. In infrared bands, angular resolution is generally much larger than typical apparent galaxy size, and hence they are essentially observed as point sources. Therefore, extended profile of galaxies is not relevant to the detection probability. However, the size of galaxies is still very important for the opacity of dust extinction. Here we summarize the modeling for galaxy sizes. We use a relation between B-band luminosity and effective radius r_e to calculate a characteristic size of a galaxy as a function of its present-day B-band luminosity. The relation between the present B luminosity L_B and effective radius r_e is assumed to be a power-law as $r_e \propto L_B^{2.5/p}$ for each galaxy type, and the normalization and

p are determined by fitting to the empirical relation observed for local galaxies. There is a considerable scatter in the empirical r_e-L_B relation (about 0.22 in $\log r_e$), and this point will also be considered later. The observed L_B-r_e relations for elliptical and spiral galaxies and fitting parameters to them can be seen in Fig. 3 of TY00. In this paper we assume that galaxy size evolves only when number evolution of galaxies takes place (see below).

A simple picture for galaxy evolution is a so-called pure luminosity evolution (PLE) model in which there is no number evolution of galaxies to high redshifts. Although some number evolution is naturally expected in the hierarchically clustering universe dominated by cold dark matter, it is very difficult to construct a realistic model of merger history of galaxies especially when one tries to predict infrared emission from dust. Therefore, we use the PLE model as our baseline model. The difficulty of modeling realistic merger history of infrared galaxies is uncertainty of size evolution of galaxies by the merger processes. In optical/NIR bands, size of galaxies is not so important when extinction is not serious and the detection incompleteness is ignored. In infrared bands, however, emission from dust is always sensitive to dust optical depth that is directly correlated with size of galaxies. Therefore size evolution induced by merging processes should have significant effect on the luminosity evolution of infrared galaxies. However, size evolution in merging galaxies is hardly understood and very difficult to construct a reliable model, even in the *ab initio* models where merging history of dark matter halos can be predicted rather well. Therefore, in this paper we will give only a simple calculation in the case of number evolution of galaxies, to grasp a rough behavior of the effects of number evolution. We introduce a simple merger model characterized by the evolution of the Schechter parameters of the luminosity function, in which total optical luminosity density is conserved, i.e., $\phi^* \propto (1+z)^\eta$ and $L_B^* \propto (1+z)^{-\eta}$. For simplicity, we assume that all types of galaxies have the same number evolution. The size evolution is determined by assuming that stellar luminosity density within a galaxy is not changed in the merger process, i.e., $L_B \propto r_e^3$. However, this is not warranted and should be considered as a simple toy model of merging galaxies.

Absorptions by interstellar dust is calculated as follows. The dust opacity is assumed to be proportional to the gas column density and metallicity, and it can be expressed by a function of restframe wavelength λ, redshift z, morphological type denoted by k, and present-day B luminosity $L_{B,0}$ as

$$\tau_{\rm d}(\lambda,z,k,L_{B,0}) = X(\lambda)A_{V,\rm MW}\left(\frac{N_{\rm gas}(z,k,L_{B,0})}{N_{\rm gas,MW}}\right)\left(\frac{Z(z,k)}{Z_{\rm MW}}\right)^s , \quad (1)$$

where $X(\lambda) = A_\lambda/A_V$ is the extinction curve, $N_{\rm gas}$ the gas column density, and Z the metallicity of interstellar gas. In this paper we use the Galactic extinction curve (e.g., Pei 1992), and $s = 1$ as a standard prescription. On the other hand, dependence of the extinction curve on metallicity can be taken into account by power-law interpolations based on the solar neighborhood and Magellanic Clouds, with $s = 1.35$ for $\lambda < 2000$Å and $s = 1.6$ for $\lambda > 2000$Å (Guiderdoni & Rocca-Volmerange 1987; Franceschini et al. 1994). We will also try this prescription later. Here the subscript MW denotes the value of the Milky Way at $z = 0$, and we assume that the Milky Way is an Sbc galaxy with $L_V = 1.4\times10^{10}L_\odot$ (Binney & Tremaine 1987). The normalization of the optical depth is fixed by the parameter $A_{V,\rm MW}$, which will be determined later. The column density can be expressed as:

$$N_{\rm gas}(z,k,L_{B,0}) \propto M_{\rm b}(k,L_{B,0})\ f_{\rm gas}(z,k)\ r_e(z,k,L_{B,0})^{-2} , \quad (2)$$

where $M_{\rm b}$ is the total baryon mass of a galaxy and $f_{\rm gas}$ the gas mass fraction. We use the present-day $L_{B,0}$ and mass-to-luminosity ratio $(M_{\rm b}/L_{B,0})_k$ given by dust-free galaxy evolution models, to calculate $M_{\rm b}$. In a strict sense, using $(M_{\rm b}/L_{B,0})$ of a dust-free evolution model is an approximation, because the observed $L_{B,0}$ is already obscured by dust. However, we use this approximation for the simplicity of numerical calculations. This approximation is reasonable provided that the optical depth of extinction at B-band in present-day galaxies is not much greater than unity, which is supported by observations for the majority of nearby galaxies. However, as we will argue, more massive or luminous galaxies are more dusty and hence the above estimate of gas column density may be underestimate for the brightest galaxies. This point will be discussed later.

Extinction of galactic light heavily depends on the spatial distribution of dust in a galaxy. Here we adopt two extreme models of spatial distribution of dust: the intervening screen model and the slab (i.e., the same distribution for stars and dust) model. The attenuation factor of galactic light is $f_{\rm att}(\lambda,z,k,L_{B,0}) = \exp(-\tau_d)$ and $\{1-\exp(-\tau_d)\}/\tau_d$ for the former and the latter, respectively. Then we obtain the extincted SED of a model galaxy as

$$L_\lambda(\lambda,z,k,L_{B,0}) = f_{\rm att}^{-1}(\lambda_B,0,k,L_{B,0})\ f_{\rm att}(\lambda,z,k,L_{B,0}) \times L_\lambda^{\rm free}(\lambda,z,k,L_{B,0}) , \quad (3)$$

where $L_\lambda^{\rm free}$ is the SED of dust-free model galaxies, and the first factor of $f_{\rm att}^{-1}$ accounts for the fact that the observed $L_{B,0}$ is already extincted. The difference between the screen and slab models is not significant for galaxies that are not so dusty (i.e., optical depth $\lesssim 1$), but is quite significant for dusty galaxies. Although the slab model seems to be more reasonable, several observations of starburst galaxies cannot be explained by the slab model. The observed correlation between power-law index of UV spectra and Balmer line ratio of starburst galaxies indicates that the observed reddening of starburst galaxies is larger than expected from the slab model, and at least some fraction of dust should behave like a screen (Calzetti, Kinney, & Storchi-Bergmann 1994, see also Gordon, Calzetti, & Witt 1997). Although the screen model may seem unreasonable, it is rather reasonable that a fraction of dust behaves like a screen with a distribution more extended than stars, since strong wind from starbursts could blow out the dust particles along with interstellar gas. This could occur in the scale of star forming regions within a galaxy and/or the whole scale of a starbursting galaxy. Some ultra luminous infrared galaxies (ULIRGs) are known to have infrared luminosity which is more than 100 times higher than optical/NIR luminosity. In the slab model, this requires an enormous amount of dust with $\tau_{\rm d} \gtrsim 100$, while in the screen model dust amount can be more modest. Therefore the screen model may be better than the slab model as a phenomenological prescription. We then use the screen model as a standard, and also use the slab model to see the dependence on the dust distributions.

The model described here has already been compared comprehensively with the counts and redshift distributions of galaxies observed in optical and NIR bands (Totani & Yoshii 2000; Totani et al. 2001c). It has been found that all data can be reasonably explained by this model assuming a Λ-dominated flat cosmology. The NIR data can be explained well by the PLE

model (Totani et al. 2001c), while the optical data suggest some modest number evolution ($\eta \sim 1$) (Totani & Yoshii 2000). The apparently discrepant results between optical and NIR bands may reflect dependence of number evolution on galaxy types, i.e., almost no number evolution for elliptical galaxies while a stronger number evolution for late-type galaxies (see Totani et al. 2001c for more detailed discussion).

3. EXTENSION TO INFRARED GALAXIES

3.1. *Determination of Effective Dust Temperature*

In the optical modeling described above, we have already calculated the absorption of stellar light by dust in a galaxy of given type at any redshift (or time). Therefore we can straightforwardly obtain the total infrared luminosity emitted by dust particles as

$$L_{\rm IR}(z,k,L_{B,0}) = \int d\lambda\ f_{\rm att}^{-1}(\lambda_B,0,k,L_{B,0}) \times [1-f_{\rm att}(\lambda,z,k,L_{B,0})]\, L_\lambda^{\rm free}(\lambda,z,k,L_{B,0})\ . \quad (4)$$

Then the task remained to predict infrared flux at a given observing band is to model the SED of dust emission. In a number of previous papers, an empirical relation between the infrared SED (or characteristic dust temperature $T_{\rm dust}$) and $L_{\rm IR}$ has been utilized here. However, as mentioned in Introduction, it is physically unreasonable to assume that the luminosity is determined by only one quantity, i.e., temperature. The total luminosity is an extensive quantity that is proportional to dust mass, provided that galaxies are transparent for dust emission. If a galaxy is simply scaled up in mass, the infrared luminosity should also increase but the temperature should not, which is an intensive quantity determined by the local physical state of dust particles. We have no reasonable physical explanation for this empirical relation so far, and it is not warranted at all that this can be applied to high-redshift galaxies.

Rather, dust temperature should be determined by an energy balance condition; i.e., temperature should be a value at which dust emissivity is consistent with total amount of stellar light absorbed by dust. We assume that total infrared luminosity is dominated by thermal radiation of big grain dust, which is well described by the so-called graybody spectrum, i.e., blackbody spectrum multiplied by the dust emissivity that is described by a power of frequency as $\epsilon \propto \nu^\gamma$, in the FIR regime. This is a good approximation for local galaxies, and we will find that it holds also for high-z galaxies whose dust temperature is higher. Then the energy balance condition can be written as:

$$L_{\rm IR} = L_{\rm IR,*}\, f_{\rm d} \left(\frac{M_{\rm dust}}{M_{\rm dust,*}}\right) \left(\frac{T_{\rm dust}}{T_{\rm dust,*}}\right)^{4+\gamma}\ , \quad (5)$$

where $M_{\rm dust}$ is the total dust mass in a galaxy and the dust emissivity index γ is typically $\gamma = 1$–2 (Boulanger et al. 1996; Hirao et al. 1996; Calzetti et al. 2000; Dunne et al. 2000). (The case of $\gamma = 0$ corresponds to the blackbody spectrum.) Throughout this paper we use $\gamma = 1.5$. The factor $f_{\rm d}$ is a mass fraction of dust heated by stellar light. In the case of the slab dust, all dust should be heated equally, while in the case of the screen dust only a part of dust can be heated by penetrating light. Therefore,

$$f_{\rm d} = \begin{cases} 1, & \text{(slab)} \\ \dfrac{1-\exp[-\tau_{\rm d}(\lambda_{\rm eff})]}{\tau_{\rm d}(\lambda_{\rm eff})}, & \text{(screen)} \end{cases} \quad (6)$$

where the characteristic wavelength $\lambda_{\rm eff}$ of absorbed stellar light is defined as:

$$\lambda_{\rm eff} = \frac{\int d\lambda\ \lambda\ [1-f_{\rm att}(\lambda)] L_\lambda^{\rm free}(\lambda)}{\int d\lambda\ [1-f_{\rm att}(\lambda)] L_\lambda^{\rm free}(\lambda)}\ . \quad (7)$$

The subscript * denotes the reference point to fix the normalization of eq. (5). We take this reference point as $L_{\rm IR,*} = 10^{10} h^{-2} L_\odot$ and $T_{\rm dust,*} = 19$ K for a galaxy type Sbc at $z = 0$, to be consistent with the observed $L_{\rm IR}$ and $T_{\rm dust}$ relation. The relative dust mass ratio ($M_{\rm dust}/M_{\rm dust,*}$) can be calculated for any model galaxy assuming that dust-to-metal ratio is constant, i.e., $M_{\rm dust} \propto f_{\rm gas} M_{\rm b} Z$. In this way we obtain $T_{\rm dust}$ for any model galaxy.

3.2. *The Infrared SED Templates*

The overall shape of a galaxy SED is basically determined by dust size spectrum and strength of radiation field. Here we should note that the entire range of infrared SED of dust emission cannot be described by a simple graybody spectrum with a single temperature. While FIR peak of the infrared SED is well described by a single-temperature graybody spectrum of cold, big grain dust, the MIR emission is dominated by radiation from heated small grains and PAHs that are not in thermal equilibrium with ambient radiation field. Because of their small heat capacity compared with the heating photon energy, these dust grains are heated stochastically by one or two photons, and their 'temperature' temporally variates violently (e.g., Purcell 1976; Draine & Anderson 1985; Siebenmorgen, Krügel, & Mathis 1992; Draine & Li 2001; Li & Draine 2001). This phenomenon makes the MIR continuum very broad, and causes a power-law like spectrum. Thus, it may be improper to describe the MIR continuum as a superposition of multi-temperature blackbody spectra.

Though the MIR continuum is dominated by the contribution from non-equilibrium dust grains, it is well correlated with temperature of big grain dust, $T_{\rm dust}$ (Shibai, Okumura, & Onaka 2000; Dale et al. 2001). It enables us to construct the overall MIR–FIR SEDs as a unique function of $T_{\rm dust}$. We utilize the observed correlations between MIR band fluxes (Dale et al. 2001) and construct the MIR regime of the model SED in an empirical way. This is a standard prescription used for the dust SED modeling in a number of previous papers. This is equivalent to assuming that the local physical state of dust particles is specified by one parameter, i.e., characteristic temperature. It is physically not unreasonable, though not warranted, to expect that this holds also for high-z galaxies, unless the composition or size distribution of dust particles in high-z galaxies is drastically different from local galaxies. The point different from previous models is that we do not simply relate $T_{\rm dust}$ to the infrared luminosity $L_{\rm IR}$, but derive $T_{\rm dust}$ by the energy balance condition.

Details of the construction of the MIR SED are as follows. The spectrum of thermal, big grain dust particles is described by a graybody spectrum with $T_{\rm dust}$. The MIR continuum coming from small particles is described by a broken power law with two different indices, which are determined by the observed flux at 12 and 25 μm compared with that in 60 μm at which the graybody is dominant. These relations are:

$$\log\frac{S_{25}}{S_{60}} = -0.026\, T_{\rm dust} + 0.367\ , \quad (8)$$

and

$$\log\frac{S_{12}}{S_{25}} = -1.75 \log\frac{S_{60}}{S_{100}} - 0.866\ , \quad (9)$$

where S_x is the flux density of infrared galaxies in units of $Wm^{-2}Hz^{-1}$ at λ = x μm, and the temperature T_{dust} is in unit of K. In addition to this, the PAH features are taken from spectroscopic data obtained by *ISO* SWS (Dale et al. 2001), and their strength is determined by the flux at 6.75 μm compared with the continuum emission as:

$$\log\frac{S_{6.75}}{S_{15}} = \begin{cases} -1.57\log S_{60}/S_{100} - 0.618 & (S_{60}/S_{100} > 0.4), \\ -0.104 & (S_{60}/S_{100} \leq 0.4). \end{cases} \quad (10)$$

Thus we obtain the MIR–FIR SEDs of galaxies with various dust temperature. Here we summarize the shape and frequency range of each component as follows: i) a power-law component (1.0×10^{12}–1.0×10^{13} [Hz]). The longer wavelength edge of this component is set to decline as a power law $\propto\nu^{2+\gamma}$, and shorter wavelength edge is set to decline exponentially. ii) a PAH continuum obeying a power law (1.0×10^{13}–3.0×10^{13} [Hz]). This component is connected to the above one smoothly. iii) a PAH band emission component (2.5×10^{13}–1.0×10^{14} [Hz]). Finally we added radio continuum to the IR SED along with the tight radio-FIR correlation (e.g. Helou, Soifer, & Rowan-Robinson 1985; Condon 1992),

$$\log S_{1.4GHz} = \log(0.867S_{60} + 0.336S_{100}) - 2.3\,. \quad (11)$$

Figure 1 shows our model SED for various values of T_{dust}. A trend is seen that the MIR component coming from nonequilibrium dust emission becomes weaker compared with the graybody emission from big grain dust, with increasing temperature. This trend is reasonable because the high temperature is equivalent to stronger flux of heating radiation field. When the heating intensity is stronger, the heating photons are more frequently absorbed by small dust grains, and hence more dust particles become in thermal equilibrium, making the spectrum closer to the graybody. There is also a large body of evidence that the PAH are likely to be destroyed, or that their emission is severely damped, in regions of high heating intensity (Dale et al. 2001 and references therein). These trends have an important implication for the compatibility of MIR CBR and TeV gamma-ray observations, which will be discussed in §6.4.

Figure 2 shows the model infrared SEDs for T_{dust} = 21 and 45 K, corresponding to the cases of the Milky Way and M82. Our model is in good agreement with the observed SEDs in both cases. Figure 3 is the same, but showing the fit of our model to other four infrared galaxies with various values of T_{dust}. These results indicate that our model of infrared SEDs is in reasonable agreement with observed infrared galaxies in a wide range of dust temperature.

Now we can predict various observable quantities of infrared galaxies, i.e., local properties as well as faint galaxy counts and CBR composed by high-redshift galaxies, based on the model of optical galaxies described in the previous section. The only one parameter not yet determined is $A_{V,MW}$, the overall normalization of dust extinction. Increasing $A_{V,MW}$ makes galaxies more dusty and hence more luminous at infrared wavebands. Infrared galaxy counts at a fixed flux then increase with $A_{V,MW}$. In this paper we set this parameter to a value at which bright infrared galaxy counts at 15, 60, and 90 μm are consistent with the *IRAS* counts (see §5.2). This is found to be $A_{V,MW}\sim0.7$ for our baseline model. However, it is important to check whether the model is consistent with observations for local infrared galaxies, before we discuss the result of counts and the CBR. This will be presented in the next section.

4. LOCAL PROPERTIES IN INFRARED: MODEL VERSUS OBSERVATIONS

Here we compare our model predictions with the properties of local galaxies observed by *IRAS*. We use the sample of the PSC*z* survey of 15411 *IRAS* galaxies selected by 60 μm flux (Saunders et al. 2000). Out of this sample, we further selected 12324 galaxies detected in the 100 μm band as well, for which the bolometric infrared luminosity can be reliably estimated. Systematic and reliable optical flux measurement is not available for all of these galaxies (see the ReadMe file of the PSC*z* catalog of Saunders et al. 2000 for detail). We use the Zwicky/RC3 magnitude as *B*-band flux, which is available for 5803 optically bright galaxies.

4.1. *Optical/Infrared Luminosity Ratio*

Figure 4 shows an L_B (νF_ν at 4400Å) versus L_{IR} (bolometric) plot. The data points are the 5803 galaxies with available *B*-band magnitudes. A clear trend can be seen that more luminous galaxies are more dusty, i.e., showing high L_{IR}/L_B ratio. On the other hand, the thick solid and dashed lines are our prediction averaged over all the four spiral galaxy types at z = 0, for the screen and slab dust, respectively. Here galaxy types are averaged by their relative proportions calculated from the type-dependent *B*-band luminosity function. It should be noted that elliptical galaxies are not included in this prediction because they do not have dust and hence infrared emission at z = 0 in our model. The trend of increasing (L_{IR}/L_B) ratio with luminosity is well reproduced by the model. This trend stems from the adopted *B* luminosity versus size relation; dust opacity, which is proportional to the metal column density, increases with L_B when the locally observed L_B-r_e relation is taken into account. Consequently, more massive galaxies emit their radiation more in infrared bands. There is a considerable scatter in the L_B-r_e relation, and this should produce scatter in the optical depth and hence a scatter along the mean L_{IR}-L_B relation. The thin-solid and thin-dashed curves are the predictions when the L_B-r_e relation is shifted by $\pm1\sigma$ = 0.223 in $\log r_e$ from the mean relation, where the line markings are the same with those of thick lines. The scatter is also in reasonable agreement with the observed scatter.

There is some offset between the prediction and mean observed L_{IR}-L_B relation. We suggest that it is due to the incompleteness of the sample; the RC3 *B*-magnitude is available only for galaxies bright in optical bands, which are about half of the whole infrared sample of 12324 galaxies. The galaxies without *B*-magnitudes are then expected to be less luminous in optical bands. This effect could lead to the lack of infrared luminous galaxies compared with the model prediction in Fig. 4.

4.2. *Dust Temperature versus Infrared Luminosity*

Figure 5 shows the infrared bolometric luminosity versus dust temperature plot. The data points are the 12324 galaxies in the *IRAS* PSC*z* sample with 100-μm flux available. Dust temperatures of the *IRAS* galaxies are estimated from their S_{60}/S_{100} flux ratio based on the temperature measurement of the Galactic dust by *IRAS* and *COBE* (Nagata et al. 2001, in preparation). The thick/thin solid and dashed lines are the model predictions, with the same line markings corresponding to model predictions shown in Fig. 4. A trend of gradual increase of mean T_{dust} with L_{IR}, as well as the scatter along the mean relation, is again well reproduced by the present model. This also stems from the fact that more luminous galaxies are more dusty, as argued in the previous subsection. This fact requires that L_{IR} should

increase faster than a simple scaling to $M_{\rm dust}$, when the mass of galaxies is increased. Considering the energy balance of $L_{\rm IR} \propto M_{\rm dust} T_{\rm dust}^{4+\gamma}$, the dust temperature must gradually increase with $M_{\rm dust}$ or $L_{\rm IR}$.

There is a clear lack of low temperature galaxies with $T_{\rm dust} \lesssim$ 16K in the *IRAS* sample. We suggest that this sudden lack may come from selection effects. As we mentioned above, the dust temperature is calculated based on the 60-μm and 100-μm fluxes. However, the sample is selected at *IRAS* 60-μm bandpass, and very cold galaxies have an IR SED peak at wavelength much longer than 60-μm. In addition, such galaxies have low luminosity in general. Therefore, cold galaxies are easily dropped by the sampling procedure in the sample used here. This is likely to be the cause of the sudden cutoff of the data on the diagram.

4.3. *Infrared Luminosity Function*

Finally we compare the model prediction of local infrared luminosity function (at 60μm) to the estimated one from observations (Saunders et al. 1990), in Fig. 6. It is well known that the infrared luminosity function is considerably different from that of optical galaxies that is well fitted by the Schechter function. The dot-dashed line is the Schechter-type luminosity function translated from the *B*-band luminosity function assuming $\nu L_\nu(B)/\nu L_\nu(60\mu{\rm m}) = 1$. In sharp contrast to the rapid exponential decline of the optical luminosity function above L^*, infrared luminosity function extends well beyond $L_{60} \sim 10^{10} L_\odot$ where L_{60} is νL_ν at 60μm (Fig. 6). Despite this intrinsic difference between the two, our model prediction with the screen dust, which is based on the *B*-band luminosity function having the Schechter form, well reproduces the shape of 60μm luminosity function up to $L_{60} \sim 10^{11} L_\odot$. Here, the infrared luminosity function is calculated as

$$\phi_{60}(L_{60}) = \sum_k \left(\frac{dM_B}{d\log_{10} L_{60}} \right)_k \phi_{B,k}(M_B) \,, \qquad (12)$$

where $\phi_{B,k}$ is the *B*-band luminosity function of the *k*-th type galaxies. This is again due to the fact that more luminous galaxies are more dusty; when optical luminosity is increased, infrared luminosity increases more rapidly than that, and hence an optical luminosity range is significantly broadened when it is translated into an infrared luminosity range. This effect is further strengthened for the infrared luminosity function at 60μm, since the gradual increase of temperature with bolometric luminosity makes the increase of 60μm luminosity even faster.

The models fail to reproduce the data at ultra-luminous region of $L \gtrsim 10^{12} L_\odot$, possibly because of the contribution of peculiar starbursting galaxies under galaxy interactions, or AGNs. In fact observations suggest that the fraction of AGNs increases with infrared luminosities (Veilleux, Kim, & Sanders 1999). Our model does not take into account these rare populations of ULIRGs at the local universe, since their contribution to counts or CBR is expected to be small (Rigopoulou et al. 2000; Barger et al. 2001). Instead, we try to explain bulk of the infrared data by the population of normal galaxies at the local universe and their ancestors at high redshifts. It should also be noted that the approximation about mass-to-light ratio ($M_{\rm b}/L_B$) breaks down for very bright and dusty galaxies, as mentioned in §2. Therefore our calculation is quantitatively unreliable and could be an underestimate at the brightest part of the infrared luminosity function.

Recently the dust mass function of local galaxies is derived by Dunne et al. (2000), based on infrared-submillimeter SEDs. They found that the dust mass function can be fitted by the Schechter function, in contrast to the 60μm luminosity function. This is also consistent with the expectation of our model; the dust mass is roughly proportional to the *B*-band luminosity unless the optical light is heavily extincted, and hence the dust mass function should be the same shape with the optical luminosity function.

5. HIGH REDSHIFT INFRARED GALAXIES

5.1. *Evolution of Infrared Luminosity and SED*

In the following part of this paper we will make predictions for high-*z* infrared galaxies such as faint galaxy counts and CBR. First we show the evolution of infrared luminosity and big-grain dust temperature ($T_{\rm dust}$) of model galaxies as a function of time after the formation in Fig. 7. These models are constructed to reproduce the observed optical SEDs and chemical properties at the typical age of present-day galaxies ($\gtrsim$10Gyr). For $T_{\rm dust}$ the three cases of dust temperature modeling are shown in the three panels: the screen dust, slab dust, and using the empirical relation between $L_{\rm IR}$ and $T_{\rm dust}$ of the local galaxies. Here, we used the best-fit relation to the observed data as:

$$T_{\rm dust} = 1.1 \log_{10}(L_{\rm IR}/L_\odot) + 8.5 \ {\rm K} \,, \qquad (13)$$

for the empirical $L_{\rm IR}$-$T_{\rm dust}$ relation (shown as a dotted line in Fig. 5). It should be noted that our evolution model depends on the mass scale of galaxies. Here we are showing the models for galaxies whose present-day *B*-band luminosity is $M_B = -20$, as typical giant galaxies. It can be seen that dust temperature evolution is much stronger than expected from the empirical $L_{\rm IR}$-$T_{\rm dust}$ relation, especially for primordial elliptical galaxies. The peak dust temperature during the starburst phase of elliptical galaxies in the slab-type dust model is $\sim$30–40K, and even higher temperature of $\sim$40–80K is found for the screen dust model, while the the empirical $L_{\rm IR}$-$T_{\rm dust}$ relation predicts $T_{\rm dust} \lesssim$ 25K in all time. This must have significant effect on the infrared SED of primordial elliptical galaxies, and hence on faint counts and CBR.

In the primordial elliptical galaxies, the dust opacity is so high and hence $\tau_{\rm d} \gg 1$ for most of optical light. Therefore, the total absorbed light, i.e., $L_{\rm IR}$ is not much different between the slab and screen models. Rather, the difference of the two mainly comes from the difference of amount of dust irradiated by stellar radiation. In the case of sceen dust model with $\tau_{\rm d} \gg 1$, only $f_{\rm d} \sim \tau_{\rm d}(\lambda_{\rm eff})^{-1}$ of total amount of dust can be heated, while all dust is heated in the slab model (eq. 6). Consequently the temperature of the screen dust model must be higher to achieve higher luminosity per unit dust mass. It should be noted that the temperature estimate in the screen model is quite robust, in a sense that it does not depend on the total amount of dust. Once $\tau_{\rm d}(\lambda_{\rm eff}) \gg 1$ is achieved, the dust-mass dependence is canceled between $f_{\rm d}$ and $M_{\rm dust}$ in the energy balance equation (eq. 5). Later, we will find that the screen model shows much better agreement with counts and CBR, than the slab model.

The high temperature which we obtained here for primordial elliptical galaxies should be compared with some observational estimates of dust temperature for high-*z* as well as local starburst galaxies. It should be noted that the dust temperature obtained from a fit to observed spectra depends on several other parameters, such as the emissivity index γ and opacity of a galaxy to FIR radiation. A same observed SED may be fitted with a higher $T_{\rm dust}$ when a smaller value of γ is assumed

or the opacity to infrared radiation ($\tau_{\rm IR}$) is significant. On the other hand, the model temperature derived here is an effective value derived from the total energy balance between dust mass and bolometric luminosity assuming $\gamma = 1.5$ and low opacity to infrared light. Therefore, our result should be compared with observational estimates of temperature derived under the same assumptions of $\gamma \sim 1.5$ and low opacity to FIR light. Keeping this point in mind, known high-z luminous starburst galaxies seem to have a mean temperature of about 50K, under the above conditions for γ and infrared opacity, and some of them show a high temperature of ~ 70K (Ivison et al. 1998a, b; Benford et al. 1999). Recently a comprehensive study for the SED of local ULIRGs is published (Klaas et al. 2001), and it again shows that the ULIRG dust temperature ranges from $\sim$40 to $\sim$80K, with $\gamma \sim 1.6$ and $\tau_{\rm IR}(100\mu{\rm m}) \sim 0.5$–5. These observations then indicate that the temperature derived by our model for primordial elliptical galaxies is in a reasonable range of typical known starburst galaxies, although it is much higher than the simple extrapolation of the mean $L_{\rm IR}$-$T_{\rm dust}$ relation of local galaxies.

5.2. *Infrared Galaxy Counts*

Figure 8 shows predictions of infrared galaxy counts compared with available data at 15, 60, 90, 170, 450, and 850 μm wavebands by our baseline model. In the baseline model, we assumed a Λ-dominated flat cosmology with $(h, \Omega_0, \Omega_\Lambda) = (0.7, 0.2, 0.8)$, formation redshift of $z_F = 3$ for all galaxy types, pure luminosity evolution without number evolution, and screen dust model. See figure caption for the references of observed data. The parameter of overall normalization of dust optical depth, $A_{V,{\rm MW}}$ is determined here so that the count predictions fit best the brightest *IRAS* counts at 15, 60, and 90 μm bands. This normalization has already been used in the previous sections. Our model predicts lower and higher counts than the bright counts observed in 15 and 60 μm, respectively, and it may suggest that our modeling of infrared SED might be imperfect, but it might also reflect some systematic uncertainties in the calibration of the observed flux in these wavebands (see e.g., Mazzei et al. 2001; Lari et al. 2001; Serjeant et al. 2001).[9] This figure shows contributions from each galaxy type as well as the total counts. Nearby spiral galaxies are dominant in the brightest counts, while contribution from elliptical galaxies rapidly appears when the flux is decreased down to a certain value, because of the strong dusty starburst of these galaxies at their formation stage. Appearance of high-z starburst galaxies revealed by SCUBA in submillimeter wavelengths is in good agreement with count predictions of forming elliptical galaxies at $z \sim 3$ in our model, and hence it can be interpreted as the emergence of forming elliptical galaxies. The redshift of $z \sim 3$ for these galaxies is also consistent with redshift estimates of SCUBA sources (e.g., Dunlop 2001). On the other hand, our model suggests that relatively weak evolution in the 15μm-band counts at $S \lesssim 10^{-2}$Jy is not due to elliptical galaxies, but induced by evolution of spiral galaxies. Strong evolution suggested by *ISO* observations (e.g., Efstathiou et al. 2000; Matsuhara et al. 2000) in the 90μm band may not be explained by the emergence of elliptical galaxies in our model. However, contribution from such galaxies with smaller z_F, or bulges of spiral galaxies, could explain the observed evolution (see Fig. 10 below). (It should be noted that the bulge and disk of spiral galaxies are modeled as a mixture in our model.)

Figures 9, 10, and 11 show the count prediction for the total of all galaxy types in cases of different cosmological models, formation redshifts, and number evolutions, respectively. The dependence on cosmological models becomes important at flux much fainter than the present sensitivity limits, except for 15μm. Therefore the uncertainty in cosmological parameters does not affect our conclusions significantly. Although there may be some uncertainties in our modeling of number evolution, it seems that the counts of SCUBA sources in submillimeter bands are better explained by primordial elliptical galaxies without number evolution, rather than the cases of number evolution. This may indicate that elliptical galaxies have formed by a single starburst at high redshifts, rather than by many starbursts of smaller building blocks which would eventually merge into a giant elliptical galaxy after the starbursts. This is consistent with a number of literature about observational constraints on number evolution of elliptical galaxies (e.g., Totani & Yoshii 1998; Im et al. 1999; Schade et al. 1999; Benitez et al. 1999; Broadhurst & Bouwens 2000; Daddi, Cimatti, & Renzini 2000; Totani et al. 2001c).

Figure 12 shows some model predictions with different model prescriptions: using empirical $L_{\rm IR}$-$T_{\rm dust}$ relation that has been used in most of previous studies (dotted line), using slab-type dust geometry rather than the screen dust (dashed), and using a different prescription for dust opacity by Guiderdoni & Rocca-Volmerange (1987) as discussed in §2, rather than assuming a constant dust-metal ratio (dot-dashed line). The last prescription gives almost the same prediction with our baseline model, and hence difference of the two prescriptions for dust/metal ratio is not important. On the other hand, the empirical $L_{\rm IR}$-$T_{\rm dust}$ relation gives quite different prediction especially for elliptical galaxies at the dusty starburst phase, because the empirical relation gives considerably lower temperature than our baseline model as shown in the previous section. Consequently, counts at 90 and 170 μm are decreased, while those at 450 and 850 μm are enhanced. The slab dust has the same effect, although it is weaker than the case of the empirical $L_{\rm IR}$-$T_{\rm dust}$ relation.

5.3. *Cosmic Background Radiation*

We show our prediction of the CBR in optical and infrared wavelengths in Fig. 13, by our baseline model whose counts have been presented in Fig. 8. The reported detections of CBR, lower limits coming from integration of galaxy counts, and upper limits on MIR CBR from TeV gamma-ray observations are also shown (see figure caption for references). The model is in overall agreement with all available data.

In optical/NIR bands, the faint-end slope of galaxy counts is very flat and hence the integration of galaxy counts with extrapolation down to even fainter magnitude is convergent. Therefore the integration of galaxy counts in these bands should not be much different from the true CBR from galaxies. Since our model is based on a model of galaxy counts in optical/NIR bands which is in agreement with observations, it is trivial that our model prediction of optical/NIR CBR is in agreement with observational estimates based on integrations of observed galaxy counts. Such estimates are shown by error bars without symbols in Fig. 13, in which the contribution to CBR by galaxies missed in deep surveys by various selection effects is taken

[9] Calibration in the MIR and FIR requires state-of-the-art techniques and especial scrutiny, and although a lot of efforts by experts have been devoted to it, there still remains a significant uncertainty. We do not go further into the problem here.

into account (Totani et al. 2001a). However, our model underpredicts the UV CBR flux compared with the observed count integrations, and this suggests that the dust extinction is too large in the model. In fact, in this paper we have set the overall normalization of dust, $A_{V,\rm MW} \sim 0.7$, so that the bright infrared galaxy counts of our model are consistent with observed data. This is considerably larger than the typical Galactic extinction in relatively high latitude, $A_{V,\rm MW} \sim 0.2$, which was used in our previous papers on optical/NIR counts (Totani et al. 2001a, b, c). This discrepancy is presumably coming from the scatter of dust optical depth in galaxies. In our model we applied a single relation between B luminosity and galaxy size for the simplicity, but in reality the scatter along the mean L_B-r_e relation should produce significant scatter of extinction, as discussed in §2 and §4. The infrared counts are expected to be dominated by galaxies with relatively large extinctions, while the optical/NIR counts, especially U band, would be dominated by those with less extinctions. This is probably the reason our prediction of UV CBR is lower than the observed count integration. Since the primary interest of this paper is in infrared bands, we will ignore the discrepancy in UV CBR in the following part of the paper.

There are several reports of detection of diffuse NIR CBR flux in the J (1.25μm), K (2.2μm) and L (3.5μm) bands as shown by diamonds in Fig. 13 (Gorjian et al. 2000; Wright & Reese 2000; Wright et al. 2001; Matsumoto et al. 2001; Cambrésy et al. 2001). All these reported diffuse NIR CBR fluxes are systematically higher by a factor of several than the integration of galaxy counts in the same bands. Our model is made to reproduce the observed galaxy counts, and hence our CBR flux agrees with the galaxy count integrations, and does not agree with the reported diffuse CBR flux. The contribution from galaxies missed in deep surveys by selection effects is very unlikely to reconcile this discrepancy (Totani et al. 2001a). It may suggest some systematic uncertainties in diffuse CBR measurements, or the contribution to the NIR CBR from yet unknown sources, but it is beyond the scope of this paper. On the other hand, there is a recent report of detection of diffuse CBR in optical bands (Bernstein, Freedman, & Madore 2002). Although the reported diffuse flux again seems higher than the count integration estimations by Totani et al. (2001a), they are consistent with each other at 1σ when all error bars (statistical and systematic of the diffuse measurements, and contribution from faint galaxies missed by deep surveys) are taken into account.

Figures 14, 15, and 16 show the CBR prediction for the total of all galaxy types in cases of different cosmological models, formation redshifts, and number evolutions, respectively. These figures show that the dependence on cosmological models or number evolution is not large compared with observational constraints, and it does not affect our conclusions significantly. On the other hand, the formation redshift can be constrained better since the sub-mm CBR flux rapidly increase with increasing z_F due to the redshift effect on the FIR peak of dust emission SED, while there is an observational constraint by COBE/FIRAS. Our model suggests that the major formation epoch of elliptical galaxies should not be larger than $z_F \sim 5$.

Figure 17 shows some model predictions with different model prescriptions, with the same models and line markings with those in Fig. 12. There is again a remarkable difference between the baseline model and the model using the empirical $L_{\rm IR}$-$T_{\rm dust}$ relation; the latter model seriously overpredicts the sub-mm CBR flux compared with the detection of the *COBE*/FIRAS. When the empirical $L_{\rm IR}$-$T_{\rm dust}$ relation is used, temperature of starbursting elliptical galaxies does not become as high as our baseline model, and hence the redshift effect significantly pushes FIR peak of CBR toward longer wavelengths. In fact, because of this reason, most of the previous papers published recently have claimed that too intense starbursts well beyond $z \sim 1$ are disfavored by the FIRAS data. However, our model suggests, based on a physical argument, that high-z starbursts of forming elliptical galaxies should have much higher temperature than previously expected from the empirical $L_{\rm IR}$-$T_{\rm dust}$ relation, and hence formation of elliptical galaxies at high redshifts ($z_F \sim 3$) with dusty starbursts is allowed, or even favored, from the data. This is consistent with the standard picture of elliptical galaxy formation (Larson 1974; Arimoto & Yoshii 1987), i.e., intense initial starburst at high redshift followed by passive evolution to the present. The screen dust model seems much better than the slab-type model, as shown in Fig. 12 and 17. This has an interesting implication for the optical/NIR colors of primordial elliptical galaxies in dusty starburst phase, and we will discuss it in the next section.

6. IMPLICATIONS AND DISCUSSION

6.1. *Forming elliptical galaxies in optical/NIR bands: HEROs*

We have shown that the screen-like dust extinction gives quantitatively much better results both for the infrared counts and CBR than the slab-like dust, if elliptical galaxies formed by starbursts at high redshifts of $z_F \gtrsim 2$ as generally believed. This is consistent with the properties of nearby starburst galaxies showing strong reddening which cannot be explained only by the slab-like dust. It also seems reasonable that at least a part of dust particles is blown out by strong galactic wind expected in the formation stage of elliptical galaxies, to have a distribution similar to a screen. An implication of this result is that forming elliptical galaxies should show very red colors when observed in optical/NIR wavelengths. When dust opacity becomes much greater than unity, colors of galaxies could infinitely increase by screen dust, while colors should reach an asymptote in the case of slab dust since emission from stars located at the outermost region becomes dominant.

In fact, such objects having unusually NIR colors of $J-K \gtrsim$ 3–4 were discovered recently in the Subaru Deep Field (Maihara et al. 2001; Totani et al. 2001b). These colors are even redder than those of typical extremely red objects (EROs) selected by optical-NIR colors, and cannot be explained by passively evolving dust-free elliptical galaxies. Totani et al. (2001b) argued that the colors, magnitudes, and counts of these enigmatic objects can be best explained by forming elliptical galaxies reddened by screen-like dust. It was also found that the surface number density of such hyper-extremely red objects (HEROs) is roughly the same with that of high-z starbursts discovered by SCUBA in sub-mm bands. In the count model of this paper, a significant part of the SCUBA sources can be explained by the forming elliptical galaxies, and hence our result here quantitatively strengthens the suggestion of Totani et al. (2001b) that the SCUBA sources and HEROs have the same origin of forming primordial elliptical galaxies in the dusty starburst phase.

6.2. *The cosmic star formation history*

Figure 18 shows the cosmic history of global star formation rate as a function of redshift, for our model as well as observational estimates coming from Hα, UV, and submillimeter lumi-

nosity density evolution. The elliptical galaxies in our model have a strong peak of SFR at their formation redshift, while the formation redshift should be distributed in some redshift range in reality. Therefore we plot the mean SFR for elliptical galaxies when they are assumed to be formed before $z = 2$ or 3, as indicated by horizontal lines.

Elliptical galaxies in our model have much higher global SFR at $z \gtrsim 3$ than the peak at $z \sim 1$ suggested by the optical observations (Lilly et al. 1996; Connolly et al. 1997; Madau, Pozzetti, & Dickinson 1998; Steidel et al. 1999; Cowie, Songaila, & Barger 1999; Thompson et al. 2001), and the model is still consistent with the FIR background detected by *COBE*/FIRAS. This is in very sharp contrast to a number of previous studies (e.g., Gispert, Lagache, & Puget 2000; Takeuchi et al. 2001a; Franceschini et al. 2001) which claimed that such high SFR beyond $z \sim 1$ is disfavored from the *COBE*/FIRAS data. This is because the dust temperature of forming elliptical galaxies is much higher than expected from the local $L_{\rm IR}$-$T_{\rm dust}$ relation, as explained in §5.3. The SFR expected from elliptical galaxies is close to those inferred from galaxies detected in submillimeter observations (Hughes et al. 1998; Barger, Cowie, & Richards 2000), and this again suggests that a considerable part of forming elliptical galaxies has been detected by submillimeter observations. [Note, however, that the higher points of Barger et al. (2000) are corrected by a factor of ~ 11 for incompleteness.] On the other hand, SFR expected from spiral galaxies is in reasonable agreement with those obtained by optical (i.e., UV in the restframe) observations. Therefore a natural interpretation of these results is that the cosmic star formation history inferred from UV light is that for steady or modest star formation in disks of spiral galaxies, while starbursts in elliptical or spheroidal components of galaxies emit their energy mostly in the form of dust emission observed in submillimeter wavelengths.

6.3. *On the origin of optical size-luminosity relation*

The key of our success to reproduce the scaling properties of local infrared galaxies (i.e., optical/infrared luminosity ratio, $L_{\rm IR}$-$T_{\rm dust}$ relation, and infrared luminosity function) is the relation between the optical luminosity and size of galaxies, which is used as an input in our model. Therefore the readers may wonder what is the origin of this relation. In fact, this scaling relation can be explained by the framework of the standard structure formation theory in the CDM universe. One can predict the virial size of cosmological objects when the mass and formation redshift are specified. Then the observed scaling relation between L_B and r_e is easily reproduced when some reasonable assumptions are made such as a roughly constant mass-to-luminosity ratio, proportionality between the virial radius and disk effective radius (equivalent to the constant angular momentum), and formation of disks at $z \lesssim 1$ (e.g., Mao & Mo 1998). The scatter along the mean relation can also be reproduced by the dispersion of angular momentum of dark haloes. This means that the local scaling relations of infrared galaxies also have their origin in the structure formation in the CDM universe. This also explains the success of a semi-analytic model of Granato et al. (2000) to reproduce the local infrared properties.

6.4. *Implications for the TeV gamma-ray observations*

TeV gamma-ray observations provide a unique constraint on CBR because very high energy gamma-rays beyond $\sim$TeV are absorbed by interaction with the infrared CBR photons to produce electron-positron pairs in intergalactic field (e.g., Gould & Schréder 1967; Stecker & de Jager 1997, 1998; Salamon & Stecker 1998; Primack et al. 1999). Gamma-rays with energy ϵ_γ mainly interact with infrared photons with wavelength $\lambda \sim h_P \epsilon_\gamma/(4m_e^2c^3) \sim 1.24\epsilon_{\gamma,\rm TeV}$ μm, where h_P is the Planck constant and $\epsilon_{\gamma,\rm TeV} = \epsilon_\gamma$/TeV. Therefore detections of gamma-rays at $\sim$ 10TeV for TeV blazars Mrk 421 ($z = 0.031$) and Mrk 501 ($z = 0.034$) (Krennrich, et al. 1999; Aharonian et al. 1999) give constraints on the MIR CBR at about 10–20 μm. The thick crosses plotted in Fig. 13 are taken from Biller et al. (1998) and Renault et al. (2001), and our baseline model is consistent with this limit. The CBR flux at 15μm in our baseline model is 2.5nW/m^2/sr, and the lower bound set by the count integration in this band accounts for about 80 % of the total CBR of the model.

It should be noted that the model using the empirical $L_{\rm IR}$-$T_{\rm dust}$ relation predicts higher MIR CBR flux, while the FIR peak is lower than the baseline model (Fig. 17). This difference originates from the dependence of MIR/FIR flux ratio of the model infrared SEDs on the dust temperature. As can be seen in Fig. 1, MIR/FIR flux ratio decreases with increasing dust temperature, due to the diminishing component of small grain dust and PAH features. This trend is physically reasonable as explained in §3.2. The difference of our baseline model and that using the empirical $L_{\rm IR}$-$T_{\rm dust}$ relation is that the dust temperature of starbursting elliptical galaxies in the former is much higher than in the latter. Therefore, in the baseline model, the strong thermal dust emission from forming elliptical galaxies has a largest contribution to the peak of FIR CBR, while it hardly contributes to the MIR CBR (Fig. 13). This is why we could reproduce simultaneously the high FIR peak and low MIR CBR flux which are fully consistent with observations of *COBE* and TeV gamma-rays.

On the other hand, the dust temperature does not become as high as our baseline model in models employing the empirical $L_{\rm IR}$-$T_{\rm dust}$ relation, and hence MIR/FIR flux ratio of CBR is not low enough to match both TeV limits in MIR and the *COBE* data in FIR. This *prima facie* conflict has been noticed in previous work based on the empirical $L_{\rm IR}$-$T_{\rm dust}$ relations of local infrared galaxies (e.g., Stecker 2000), and several possibilities have been proposed to solve this conflict, including new physics such as a possibility of the broken Lorentz invariance. However, our model suggests that the MIR and FIR CBR are made by completely different populations of galaxies: low-redshift spiral galaxies for MIR while high-redshift starbursting elliptical galaxies for FIR, as seen in Fig. 13. Thus in our model the conflict is naturally resolved.

We calculated the optical depth of TeV gamma-rays as a function of source redshift (z_s) and gamma-ray energy observed at $z = 0$, based on the formulations given in Salamon & Stecker (1998). The result is shown in Fig. 19, along with the previous calculations of Stecker & de Jager (1998, hereafter SD98) based on the empirical $L_{\rm IR}$-$T_{\rm dust}$ relation. The baseline model is used for the flux and its evolution of the CBR from optical to FIR. As expected, the optical depth of our model (indicated as TTTTT in the figure from the initials of the authors) is relatively smaller at gamma-ray energies of $\sim$ 1–10 TeV where the main target photons are in the MIR band, while it becomes larger for higher energy gamma-rays interacting with FIR photons, when compared with the SD98 calculation. The different two models might be discriminated by more accurate measurement of the

TeV spectrum of Mrk 421 and/or 501 in future observations. Following SD98, we give the result of polynomial fits to the optical depth $\tau(z_s, \epsilon_\gamma)$, as

$$\tau(z_s, \epsilon_\gamma) = \sum_{0 \le i \le 3} \sum_{0 \le j \le 2} a_{ij} (\log_{10} \epsilon_{\gamma,\mathrm{TeV}})^i (\log_{10} z_s)^j \ , \qquad (14)$$

where the values of a_{ij} are presented in Table 1. This fitting formula gives a reasonable approximation ($< 10\%$ at $z_s = 0.03$ and $1 < \epsilon_{\gamma,\mathrm{TeV}} < 20$, and $\lesssim 50\%$ within ranges of $0.03 < z_s < 0.3$ and $0.1 < \epsilon_{\gamma,\mathrm{TeV}} < 50$). More accurate table of the optical depth with wider ranges of z_s and ϵ_γ is available on request to the authors.

7. SUMMARY AND CONCLUSIONS

In this paper we developed a new model of counts and cosmic background radiation (CBR) of infrared galaxies observed by emission from heated interstellar dust, by extending a model for optical/NIR galaxies (Totani & Yoshii 2000). Five morphological types of galaxies (E/S0, Sab, Sbc, Scd, and Sdm) are taken into account and their number densities are normalized by type-dependent *B*-band luminosity function at the local universe. Their luminosity evolution is traced backwards in time based on star formation histories inferred from the present-day optical/NIR SEDs and chemical properties. Formation epoch of galaxies is a parameter for which we tried a redshift range of $2 \le z_F \le 5$. Pure luminosity evolution without number evolution is assumed in our baseline model, but some number evolution is also tested in a phenomenological way. The model has already been compared comprehensively with the counts and redshift distributions of galaxies observed in optical and NIR bands, and found to be in reasonable agreement with the data (Totani & Yoshii 2000; Totani et al. 2001c).

Relatively rare populations of AGNs and ULIRGs seen in the local universe, whose contribution to counts and CBR is expected to be small, are not included in our model, and we tried to explain the bulk of infrared data by normal galaxy populations at the local universe and their ancestors at high redshifts. On the other hand, our analysis strongly indicates that the primordial elliptical galaxies are very similar to dusty starburst galaxies or ULIRGs with very high dust temperature.

There are two important new characteristics in our model that are different from previous models of infrared galaxies: (1) mass scale dependence of dust extinction is introduced by the observed size-luminosity relation of optical galaxies, and (2) dust temperature is determined by physical consideration of energy balance, rather than using the empirical relation between the total infrared luminosity (L_{IR}) and characteristic dust temperature (T_{dust}) of local galaxies that has been used in a number of previous models. As a result, the local properties of infrared galaxies, such as optical/infrared luminosity ratios, correlation between infrared luminosity and dust temperature, and infrared luminosity function, are outputs that should be compared with observed data. Indeed we found that our model quantitatively reproduces the observed infrared properties at the local universe. The key to understand these scaling properties is the size-luminosity relation of galaxies; surface brightness and dust column density increase with increasing optical galaxy luminosity, and hence more massive galaxies should be more dusty. This gives a quantitative explanation for the observed correlation between optical and infrared luminosities. Furthermore, massive galaxies should emit more energy as dust emission per unit mass of dust, and hence the energy balance inevitably results in higher temperature for larger galaxies, as observed for local infrared galaxies. The scatter along the mean L_B-r_e relation is comparable with those in L_{IR}-L_B and L_{IR}-T_{dust} relations. These effects result in much faster increase of 60μm luminosity when L_B is increased, and giving an explanation for the much broader shape of 60μm luminosity function than the Schechter function of the optical luminosity function.

Then we predicted faint source counts and CBR composed of high-z galaxies. Our baseline model assumes a cosmological model with $(h, \Omega_0, \Omega_\Lambda) = (0.7,\ 0.2,\ 0.8)$, pure luminosity evolution after formation at $z_F = 3$, and screen distribution of dust. We found that this baseline model is in reasonable agreement with all available data of galaxy counts in six wavebands (15, 60, 90, 170, 450, and 850μm) and CBR. Therefore our model, based only on present-day normal galaxy populations and their evolution, reasonably fits to all available data from optical to submillimeter wavebands, though some modest number evolution may be required for late-type galaxies. The high-z starburst galaxies discovered by SCUBA are quantitatively well explained in our model by the emergence of starbursts at the formation of present-day elliptical galaxies at $z \sim 3$.

We also tested that slab-type dust distribution as well as the screen dust used in the baseline model, and found that the screen model gives much better fit to the observed data of the local infrared luminosity function, galaxy counts, and CBR. Although a pure screen distribution may seem unlikely, it is rather reasonable to expect that a part of dust particles behave like an effective screen, because of stellar/galactic wind or inhomogeneity of interstellar medium. If it is the case, and the dust opacity to optical/NIR is much larger than the unity, the screen model should be better than the slab-type prescription. It is also supported by extremely red colors of local starburst galaxies (Calzetti, Kinney, & Storchi-Bergmann 1994) or recently discovered hyper extremely red objects (Totani et al. 2001b), which cannot be explained simply by slab-type dust. Therefore we conclude that screen dust is a better phenomenological description than slab dust at least in a study of this kind.

The most drastic difference of our model from previous ones is that the dust temperature of starbursting elliptical galaxies is predicted to be much higher ($\sim$ 40–80K) than that extrapolated by the empirical L_{IR}-T_{dust} relation of local infrared galaxies. This is because starbursting elliptical galaxies should emit much larger amount of energy as dust emission *per unit dust mass*, than local galaxy populations. On the other hand, such high temperature is similar to those found in local ULIRGs or high-z dust starbursts observed in sub-mm bands. Thus, our result gives a further support to an idea that the progenitor of present-day elliptical galaxies or bulges are dusty starbursts.

There is an important implication for the cosmic star formation history, which is very different from previous results. A number of papers based on the empirical L_{IR}-T_{dust} relation claimed that cosmic star formation rate beyond $z \gtrsim 1$ must turn over and keep constant or decline, otherwise it would produce too much submillimeter CBR compared with the *COBE*/FIRAS data, by the redshifted dust emission from high-z galaxies (e.g., Gispert, Lagache, & Puget 2000; Takeuchi et al. 2001a; Franceschini et al. 2001). However, in our model the dust temperature of forming elliptical galaxies is much higher than in the previous models. As a result, although our model assumes very strong starbursts at $z_F \sim 3$ in primordial elliptical galaxies and the cosmic SFR at $z_F \gtrsim 2$–3 is even higher than the peak at $z \sim 1$ suggested by optical observations, the prediction is in good agreement not only with the *COBE*/FIRAS CBR measurements

but also with the counts and redshift estimation for submillimeter sources revealed by SCUBA. In our model the dusty starbursts in primordial elliptical galaxies hardly contribute to the cosmic SFR measured by optical observations.

Another result that is significantly different from previous studies is the smaller ratio of MIR/FIR CBR flux compared with models based on the empirical $L_{\rm IR}$-$T_{\rm dust}$ relation of local infrared galaxies (e.g., Stecker 2000). It should be noted that our model does include the warm/nonequilibrium components of dust emission that dominate the thermal emission from big grain dust at the MIR region, while several previous models gave very low MIR CBR flux as a valley in the CBR spectrum simply because they did not take them into account (e.g., MacMinn & Primack 1996; Fall, Charlot, & Pei 1996). The reason we get this result is the trend that the warm/nonequilibrium components become less significant compared with thermal big-grain dust emission, with increasing temperature of dust. This is inferred from the infrared spectrum of local galaxies, and it is also expected from physical consideration. If this trend is taken for granted for high-z galaxies, the MIR/FIR flux ratio of dust emission from forming elliptical galaxies should be much smaller than that of local infrared galaxies, since the dust temperature of starbursting elliptical galaxies is found to be very high in our model. Therefore these galaxies dominate in the FIR peak of CBR while they have very small contribution in MIR CBR. This effect is significant enough to resolve the *prima facie* conflict (Stecker 2000) between the upper limits on MIR CBR from TeV gamma-ray observations and FIR CBR detections by *COBE*/DIRBE and FIRAS.

The authors have financially been supported by the JSPS Fellowship. The authors thank Hirohisa Nagata for providing their temperature data of *IRAS* galaxies.

REFERENCES

Aharonian, F. et al. 1997, A&A 327, L5
Aharonian, F. et al. 1999, A&A 342, 69
Altieri, B., Metcalfe, L., Kneib, J. -P., McBreen, B., Aussel, H., Biriano, A., Delaney, M., Elbaz, D., et al. 1999, A&A, 343, L65
Arimoto, N., & Yoshii, Y. 1987, A&A, 173, 23
Arimoto, N., Yoshii, Y., & Takahara, F. 1992, A&A, 253, 21
Armand, C., Milliard, B., & Deharveng J. M. 1994, A&A 284, 12
Aussel, H., Césarsky, C., Elbaz, D., & Starck, J. L. 1999, A&A, 342, 313
Barger, A. J., Cowie, L. L., Sanders, D. B., Fulton, E., Taniguchi, Y., Sato, Y., Kawara, K., & Okuda, H. 1998, Nature, 394, 248
Barger, A. J., Cowie, L. L., & Sanders, D. B. 1999, ApJ, 518, L5
Barger, A.J., Cowie, L.L., & Richards, E.A. 2000, AJ, 119, 2092
Barger, A. J., Cowie, L. L., Mushotzky, R. F., & Richards, E. A. 2001, AJ, 121, 662
Beichman, C. A. & Helou, G. 1991, ApJ, 370, L1
Benford, D.J., Cox, P., Omont, A., Phillips, T.G., McMahon, G. 1999, ApJ, 518, L65
Benitez, N., Broadhurst, T.J., Bouwens, R.J., Silk, J., & Rosati, P. 1999, ApJ, 515, L65
Biller, S.D., et al. 1998, Phys. Rev. Lett. 80, 2992
Binney, J. & Tremaine, S. 1987, Galactic Dynamics, Princeton University Press
Blain, A. W. & Longair, M. S. 1993, MNRAS, 264, 509
Blain, A. W. & Longair, M. S. 1996, MNRAS, 279, 847
Blain, A. W., Kneib, J. -P., Ivison, R. J., & Smail, I. 1999, ApJ, 512, L87
Blain, A. W., Ivison, R. J., Kneib, J. -P., & Smail, I. 2000, in The Hy-Redshift Universe, ed A. J. Bunker, & W. J. M. van Breugel, ASP Conf. Ser. vol.193, San Francisco: ASP, p246
Boulanger, F., Abergel, A., Bernard, J.-P., Burton, W. B., Désert, F.-X., Hartmann, D., Lagache, G., & Puget, J.-L. 1996, A&A, 312, 256
Broadhurst, T.J. & Bouwens, R.J., 2000, ApJ, 530, L53
Calzetti, D. A., Kinney, A. L., & Storchi-Bergmann, T. 1994, ApJ, 429, 582
Calzetti, D., Armus, L., Bohlin, R. C., Kinney, A. L., Koornneef, J., & Storchi-Bergmann, T. 2000, ApJ, 533, 682
Cambrésy, L., Reach, W. T., C.A. Beichman, T. H. Jarrett, 2001, ApJ, 555, 563
Clements, D. L., Desert, F. X., Franceschini, A., Reach, W. T., Baker, A. C., Davies, J. K., & Césarsky, C. 1999, A&A, 346, 383
Cole, S., Aragon-Salamanca, A., Frenk, C. S., Navarro, J. F., & Zepf, S.E. 1994, MNRAS, 271, 781
Cole, S., Lacey, C. G., Baugh, C. M., Frenk, C. S. 2000, MNRAS, 319, 168
Condon, J. J. 1992, ARA&A, 30, 575
Connolly, A. J., Szalay, A. S., Dickinson, M., Subba Rao, M. U., & Brunner, R. J. 1997, ApJ, 486, L11
Cowie, L.L., Songaila, A., & Barger, A.J. 1999, AJ, 118, 603
Daddi, E., Cimatti, A., & Renzini, A. 2000, A&A 362, L45
Dale, D. A., Helou, G., Contursi, A., Silbermann, N. A., & Kolhatkar, S. 2001, ApJ, 549, 215
Devriendt, J. E. G. & Guiderdoni, B. 2000, A&A, 363, 851
Dole, H. et al. 2001, A&A, 372 364
Draine, B. T., & Anderson, L. 1985, ApJ, 292, 494
Draine, B. T. & Li, A. 2001, ApJ, 551, 807
Dunlop, J. S. 2001, New Astronomy Reviews, in press (astro-ph/0101297)
Dunne, L., Eales, S.,Edmunds, M., Ivison, R., Alexander, P., & Clements, D. L. 2000, MNRAS, 315, 115
Dwek, E., Arendt, R. G., Fixsen, D. J., Sodroski, T. J., Odegard, N., Weiland, J. L., Reach, W. T., Hauser, M. G., et al. 1997, ApJ, 475, 565
Dwek, E., et al. 1998, ApJ, 508, 106
Eales, S., Lilly, S., Gear, W., Dunne, L., Bond, J. R., Hammer, F., Le Fèvre, O., & Crampton, D. 1999, ApJ, 515, 518
Eales, S., Lilly, S., Webb, T., Dunne, L., Gear, W., Clements, D., & Yun, M. 2000, AJ, 120, 2244
Elbaz, D., Cesarsky, C. J., Fadda, D., Aussel, H., Désert, F. X., Franceschini, A., Flores, H., Harwit, M., et al. 1999, A&A, 351, L37
Efstathiou, A. et al. 2000, MNRAS, 319, 1169
Fall, S. M., Charlot, S., & Pei, Y.C. 1996, ApJ 464, L43
Fixsen, D. J., et al. 1998, ApJ, 508, 123
Flores, H., Hammer, F., Désert, F. X., Césarsky, C., Thuan, T., Crampton, D., Eales, S., Le Fèvre, O., et al. 1999a, A&A, 343, 389
Flores, H., Hammer, F., Thuan, T. X., Césarsky, C., Desert, F. X., Omont, A., Lilly, S. J., Eales, S., Crampton, D., & Le Fèvre, O. 1999b, ApJ, 517, 148
Franceschini, A., Mazzei, P., de Zotti, G., & Danese, L. 1994, ApJ, 427, 140
Franceschini, A., Aussel, H., Cesarsky, C. J., Elbaz, D., & Fadda, D. 2001, A&A, 378, 1
Frayer, D. T., Ivison, R. J., Smail, I., Yun, M. S., & Armus, L. 1999, AJ, 118, 139
Bernstein, R.A., Freedman, W.L., & Madore, B.F. 2002, ApJ in press, astro-ph/0112170
Fukugita, M., Takahara, F., Yamashita, K., & Yoshii, Y. 1990, ApJ, 361, L1
Gallego, J., Zamorano, J., Aragon-Salamanca, A., & Rego, M. 1995, ApJ, 455, L1 (erratum: 459, L43)
Genzel, R., & Cesarsky, C. J. 2000, ARA&A, 38, 761
Gispert, R., Lagache, G., & Puget, J.-L. 2000, A&A, 360, 1
Gordon, K. D., Calzetti, D., & Witt, A. N. 1997, ApJ, 487, 625
Gorjian, V., Wright, E. L., & Chary, R. R. 2000, ApJ 536, 550
Gould, R. P. & Schréder, G. P., 1967, Phys. Rev. 155, 1408
Granato, G. L., Lacey, C. G., Silva, L., Bressan, A., Baugh, C. M., Cole, S., & Frenk, C. S. 2000, ApJ, 542, 710
Guiderdoni, B., & Rocca-Volmerange, B. 1987, A&A, 186, 1
Guiderdoni, B., Hivon, E., Bouchet, F. R., & Maffei, B. 1998, MNRAS, 295, 877
Hauser, M. G., et al. 1998, ApJ, 508, 25
Helou, G., Soifer, B. T., & Rowan-Robinson, M. 1985, ApJ, 298, L7
Hirao, T., Matsumoto, T., Sato, S., Ganga, K., Lange, A. E., Smith, B. J., & Freund, M. M. 1996, PASJ, 48, L77
Holland, W. S., Robson, E. I., Gear, W. K., Cunningham, C. R., Lightfoot, J. F., Jenness, T., Ivison, R. J., Stevens, J. A., et al. 1999, MNRAS, 303, 659
Hughes, D. H. et al. 1998, Nature, 394, 241
Im, M., Griffiths, R.E., Naim, A., Ratnatunga, K.U., Roche, N., Green, R.F., & Sarajedini, V.L. 1999, ApJ 510, 82
Ivison, R.J. et al. 1998a, ApJ, 494, 211
Ivison, R.J., Smail, I., Le Borgne, J.-F., Blain, A.W., Kneib, J.-P., Bézecourt, J., Kerr, T.H., & Davies, J.K. 1998b, MNRAS, 298, 583
Jimenez, R. & Kashlinsky, A. 1999, ApJ, 511, 16
Juvela, M., Mattila, K., & Lemke, D. 2000, A&A, 360, 813
Kawara, K., Sato, Y., Mastuhara, H., Taniguchi, Y., Okuda, H., Sofue, Y., Matsumoto, T., Wakamatsu, K., et al. 1998, A&A, 336, L9
Kauffmann, G., White, S. D. M., & Guiderdoni, B. 1993, MNRAS, 264, 201
Klaas, U., Haas, M., Heinrichsen, I., & Schulz, B. 1997, A&A, 325, L21
Klaas, U., et al. 2001, A&A, 379, 823
Krennrich, F. et al. 1999, ApJ, 511, 149
Lagache, G., Haffner, L. M., Reynolds, R. J., & Tufte, S. L. 2000, A&A, 354, 247
Lari, C., Pozzi, F., Gruppioni, C., Aussel, H., Ciliegi, P., Danese, L., Franceschini, A., Oliver, S., Rowan-Robinson, M., & Serjeant, S. 2001, MNRAS, 325, 1173
Larson, R. B. 1974, MNRAS, 166, 686
Li, A., & Draine, B. T. 2001, ApJ, 554, 778
Lilly, S. J., Le Fèvre, O., Hammer, F., & Crampton, D. 1996, ApJ, 460, L1

Lonsdale, C. J., Hacking, P. B., Conrow, T. P., & Rowan-Robinson, M. 1990, ApJ, 358, 60
Madau, P., Pozzetti, L., & Dickinson, M. 1998, ApJ, 498, 106
MacMinn, D. & Primack, J. R. 1996, Sp. Sci. Rev. 75, 413
Maihara, T. et al. 2001, PASJ, 53, 25
Malkan, M. A. & Stecker, F. W. 1998, ApJ, 496, 13
Malkan, M. A. & Stecker, F. W. 2001, ApJ, 555, 641
Mao, S. & Mo, H. J. 1998, MNRAS, 296, 847
Martin, C., Hurwitz, M., & Bowyer, S. 1991, ApJ, 379, 549
Marzke, R. O., da Costa, L. N., Pellegrini, P. S., Willmer, C. N. A., & Geller, M. J. 1998, ApJ, 503, 617
Matsuhara, H., et al. 2000, A&A, 361, 407
Matsumoto, T. et al. 2000, in ISO Surveys of a Dusty Universe, ed D. Lemke, M. Stickel, & K. Wilke, Heidelberg: Springer, p96
Mazzei, P., Aussel, H., Xu, C., Salvo, M., De Zotti, G., & Franceschini, A. 2001, NewA, 6, 265
Nagashima, M., Totani, T., Gouda, N., & Yoshii, Y. 2001, ApJ 557, 505
Okuda, H. 2000, in ISO Surveys of a Dusty Universe, ed D. Lemke, M. Stickel, & K. Wilke, Heidelberg: Springer, p40
Oliver, S. J., Rowan-Robinson, M., & Saunders, W. 1992, MNRAS, 256, L15
Oliver, S., Goldshmidt, P., Franceschini, A., Serjeant, S. B. G., Efstathiou, A., Verma, A., Gruppioni, C., Eaton, N., et al. 1997, MNRAS, 289, 471
Oliver, S., et al. 2000, MNRAS, 316, 749
Pearson, C. & Rowan-Robinson, M. 1996, MNRAS, 283, 174
Pei, Y. C. 1992, ApJ, 395, 130
Pei, Y. C. & Fall, S. M. 1995, ApJ, 454, 69
Pei, Y. C., Fall, S. M., & Hauser, M. G. 1999, ApJ, 522, 604
Pozzetti, L., Bruzual, G. A., & Zamorani, G. 1996, MNRAS, 281, 953
Pozzetti, L., Madau, P., Zamorani, G., Ferguson, H. C. & Bruzual, C. A. 1998, MNRAS 298, 1133
Primack, J. R., Bullock, J. S., Somerville, R. S., & MacMinn, D. 1999, Astropart. Phys., 11, 93
Puget, J. -L., Abergel, A., Bernard, F., Boulanger, F., Burton, W. B., Desert, F. -X., & Hartmann, D. 1999, A&A, 345, 29
Purcell, E. M. 1976, ApJ, 206, 685
Renault, C., Barrau, A., Lagache, G., & Puget, J.-L. 2001, A&A, 371, 771
Rigopoulou, D. et al. 2000, ApJ, 537, L85
Rocca-Volmerange, B. & Guiderdoni, B. 1990, MNRAS, 247, 166
Roche, N. & Eales, S. A. 1999, MNRAS, 307, 111
Rowan-Robinson, M., Saunders, W., Lawrence, A., & Leech, K. 1991, MNRAS, 253, 485
Rush, B., Malkan, M. A., & Spinoglio, L. 1993, ApJS, 89, 1
Sadat, R., Guiderdoni, B., & Silk, J. 2001, A&A, 369, 26
Salamon, M. H. & Stecker, F. W. 1998, ApJ, 493, 547
Saunders, W., Rowan-Robinson, M., Lawrence, A., Efstathiou, G., Kaiser, N., Ellis, R. S., & Frenk, C. S. 1990, MNRAS, 242, 318
Saunders, W., et al. 2000, MNRAS, 317, 55
Schade, D. et al. 1999, ApJ, 525, 31
Serjeant, S., et al. 2000, MNRAS, 316, 768
Shibai, H., Okumura, K., & Onaka, T. 2000, in Star Formation 1999, ed. T. Nakamoto (Nobeyama Radio Observatory: NRO)
Siebenmorgen, R., Krügel, E., & Mathis, J. S. 1992, A&A, 266, 501
Smail, I., Ivison, R. J., & Blain, A. W. 1997, ApJ, 490, L5
Smith B. J., Kleinman, S. G., Huchra, J. P., & Low, F. J. 1987, ApJ, 318, 161
Soifer B. T., & Neugebauer, G. 1991, AJ, 101, 354
Soifer, B. T., Houck, J. R. & Neugebauer, G. 1987, ARA&A, 25, 187
Somerville, R. S. & Primack, J. R. 1999, MNRAS, 310, 1087
Stecker, F. W. & de Jager, O. C. 1997, ApJ, 476, 712
Stecker, F. W. & de Jager, O. C. 1998, A&A, 334, L85
Stecker, F. W. 2000, in the extragalactic infrared background and its cosmological implications, IAU symposium, Vol. 204, 2000, eds. M. Harwit and M.G. Hauser (astro-ph/0010015)
Steidel, C. C., Adelberger, K. L., Giavalisco, M., Dickinson, M., Pettini, M. 1999, ApJ, 519, 1
Stickel, M., Bogun, S., Lemke, D., Klaas, U., Tóth, L. V., Herbstmeier, U., Richter, G., Assendorp, R., et al. 1998, A&A, 336, 116
Takeuchi, T. T., Hirashita, H., Ohta, K., Hattori, T. G., Ishii, T. T. & Shibai, H. 1999, PASP, 111, 288
Takeuchi, T. T., Ishii, T. T., Hirashita, H., Yoshikawa, K., Matsuhara, H., Kawara, K., & Okuda, H. 2001a, PASJ, 53, 37
Takeuchi, T. T., Kawabe, R., Kohno, K., Nakanishi, K., Ishii, T. T., Hirashita, H., & Yoshikawa, K. 2001b, PASP, 113, 586
Tan, J. C., Silk, J., & Balland, C. 1999, ApJ, 522, 579
Thompson, R.I., Weymann, R.J., & Strorrie-Lombardi, L.J. 2001, ApJ, 546, 694
Thuma, G., Neininger, N., Klein, U., & Wielebinski, R. 2000, A&A, 358, 65
Tinsley, B. M. 1980, Fund. Cosmic Phys., 5, 287
Totani, T. & Yoshii, Y. 1998, ApJ, 501, L177
Totani, T. & Yoshii, Y. 2000, ApJ, 540, 81 (TY00)
Totani, T., Yoshii, Y., Iwamuro, F., Maihara, T., & Motohara, K. 2001a, ApJ, 550, L137
Totani, T., Yoshii, Y., Iwamuro, F., Maihara, T., & Motohara, K. 2001b, ApJ, 558, L87
Totani, T., Yoshii, Y., Iwamuro, F., Maihara, T., & Motohara, K. 2001c, ApJ, 559, 592
Tresse, L. & Maddox, S. 1998, ApJ, 495, 691
Treyer, M. A., Ellis, R. S., Milliard, B., Donas, J., & Bridges, T. J. 1998, MNRAS, 300, 303
Veilleux, S., Kim, D.-C., & Sanders, D. B. 1999, ApJ, 522, 113
Wang, Y. P., & Biermann, P. L. 2000, A&A, 358, 409
Williams, R. T. et al. 1996, AJ, 112, 1335
Williams, R. T. et al. 2000, AJ, 120, 2735
Wright, E. L. & Reese, E. D. 2000, ApJ, 545, 43
Wright, E. L. 2001, ApJ, 553, 538
Xu, C., Lonsdale, C. J., Shupe, D. L., O'Linger, J., & Masci, F. 2001, ApJ, in press (astro-ph/0009220)
Yoshii, Y. & Peterson, B.A. 1991, ApJ, 372, 8
Yoshii, Y. 1993, ApJ, 403, 552
Yoshii, Y. & Peterson, B.A. 1995, ApJ, 444, 15
Yoshii, Y. & Takahara, F. 1988, ApJ, 326, 1
Yun, M. S., Carilli, C. L., Kawabe, R., Tutui, Y., Kohno, K., & Ohta, K. 2000, ApJ, 528, 171

TABLE 1
POLYNOMIAL FITS TO $\tau(\epsilon_\gamma, z_s)$

j	a_{0j}	a_{1j}	a_{2j}	a_{3j}
0	1.11	0.85	–0.28	0.32
1	1.16	0.42	0.87	–0.53
2	0.04	0.21	0.35	–0.23

Note.— This fitting formula is accurate within 10% at $z_s = 0.03$ and $1 \leq \epsilon_\gamma \leq 20$, and within $\sim 50\%$ for ranges of $0.03 \leq z_s \leq 0.3$ and $0.1 \leq \epsilon_\gamma \leq 50$ TeV.

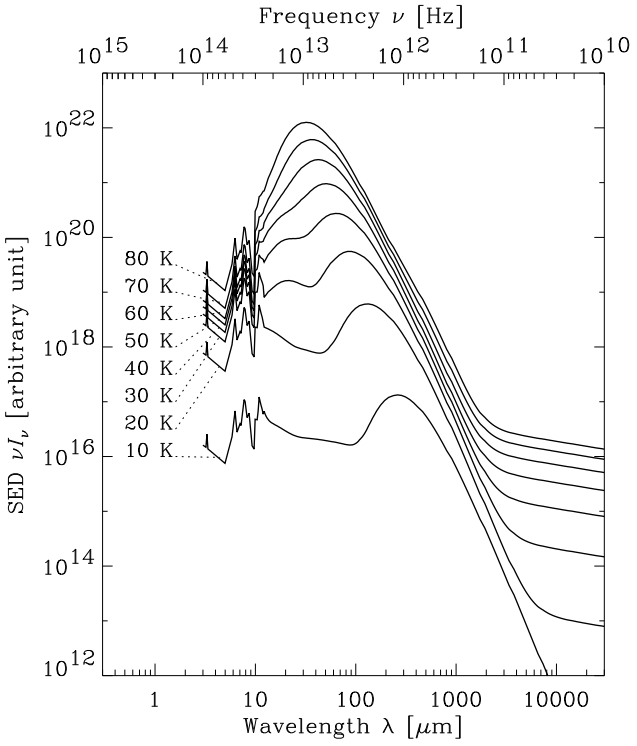

FIG. 1.— The infrared spectral energy distribution (SED) of model galaxies, for various values of the temperature of big grain dust in thermal equilibrium (indicated in the figure). The nonthermal emission coming from small grain dust and PAH features are also taken into account.

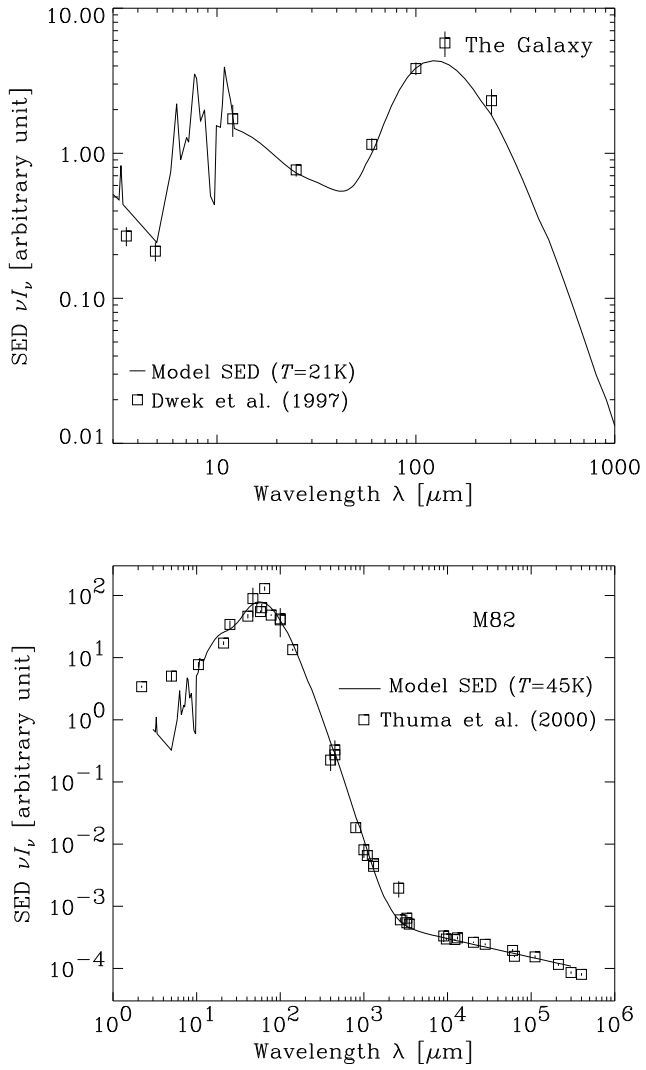

FIG. 2.— Infrared spectral energy distribution (SED) of the Milky Way (top panel) and M82 (bottom panel). The model curves are fit by our model SED described by a characteristic temperature of cold, big grain dust (indicated in the panels), while the nonthermal emission coming from small grain dust and PAH features are also added. The observed data are from Dwek et al. (1997) for the Milky Way, and Thuma et al. (2000) for M82.

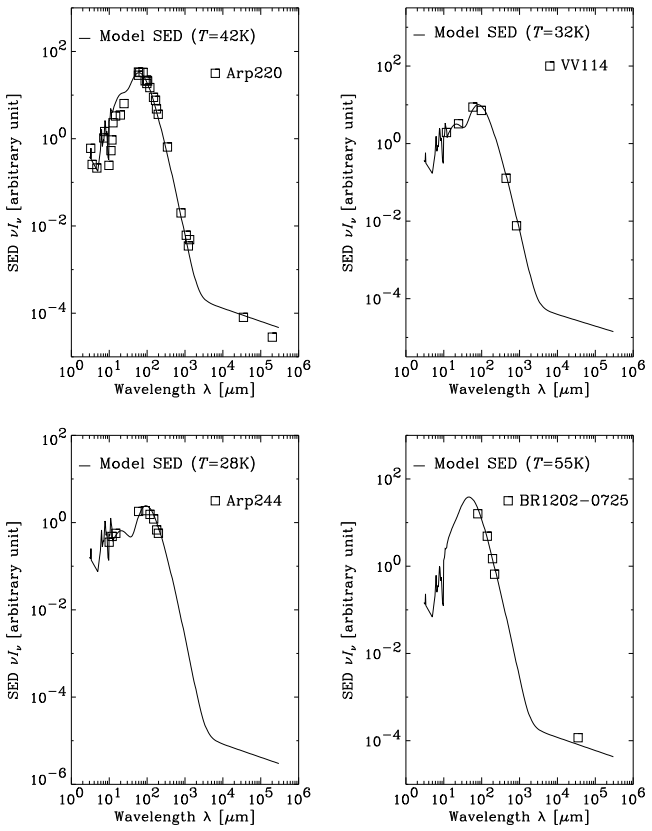

FIG. 3.— The same as Fig. 2, but for other four nearby infrared galaxies. The observed data are taken from Klaas et al. (1997) for Arp 220 and Arp 244, Frayer et al. (1999) for VV 114, and Yun et al. (2000) for BR 1202–0725, respectively.

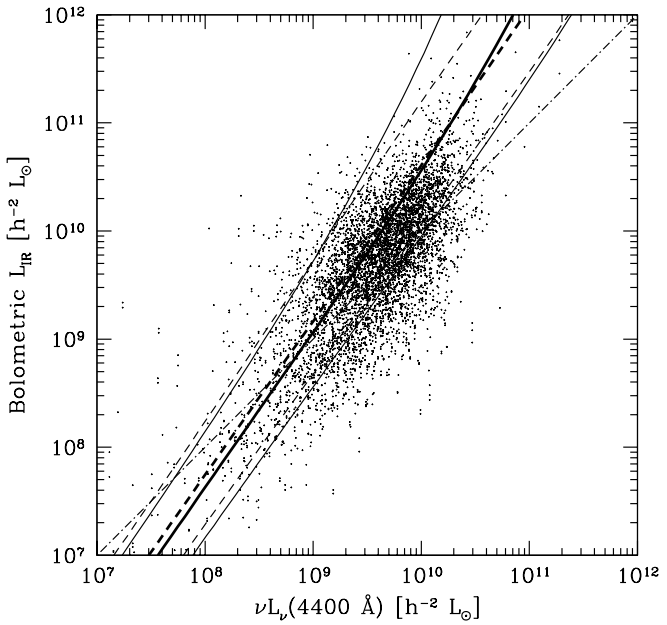

FIG. 4.— Correlation plot of the bolometric infrared luminosity versus optical luminosity (B-band) of galaxies. The data are from Saunders et al. (2000). The dot-dashed line is that corresponds to $L_{\rm IR}/\nu L_\nu(B) = 1$. The thick solid and dashed lines are the prediction of our model assuming the screen and slab distribution of dust, respectively. The thin solid and dashed lines are the same with the thick lines, but in the cases where the size of galaxies are shifted by $\pm 1\sigma$ of observed dispersion in $\log r_e$.

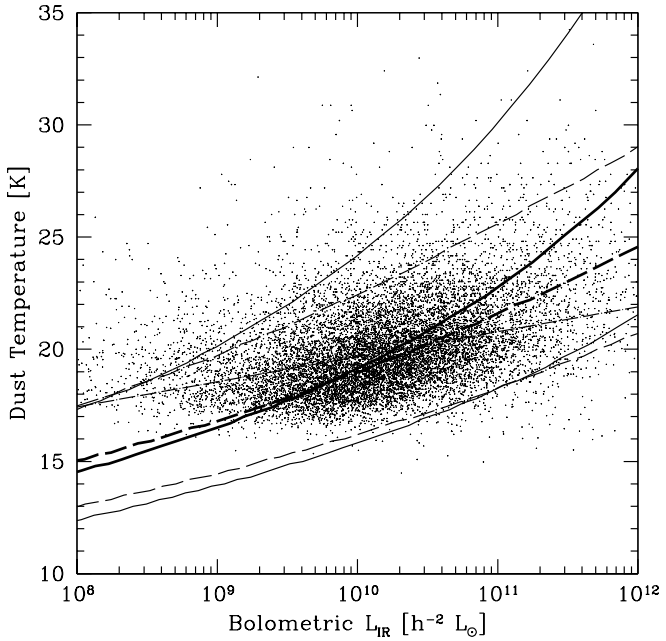

FIG. 5.— Correlation plot of the bolometric infrared luminosity versus temperature of cold, big grain dust estimated from 60 and 100 μm fluxes. The data are taken from Saunders et al. (2000). The thick solid and dashed lines are the prediction of our model assuming the screen and slab distribution of dust, respectively. The thin solid and dashed lines are the same with the thick lines, but in the cases where the size of galaxies are shifted by $\pm 1\sigma$ of observed dispersion in $\log r_e$. The dot-dashed line is a simple linear fit to the data, which is used to determine the dust temperature based on the empirical $L_{\rm IR}$-$T_{\rm dust}$ relation (eq. 13).

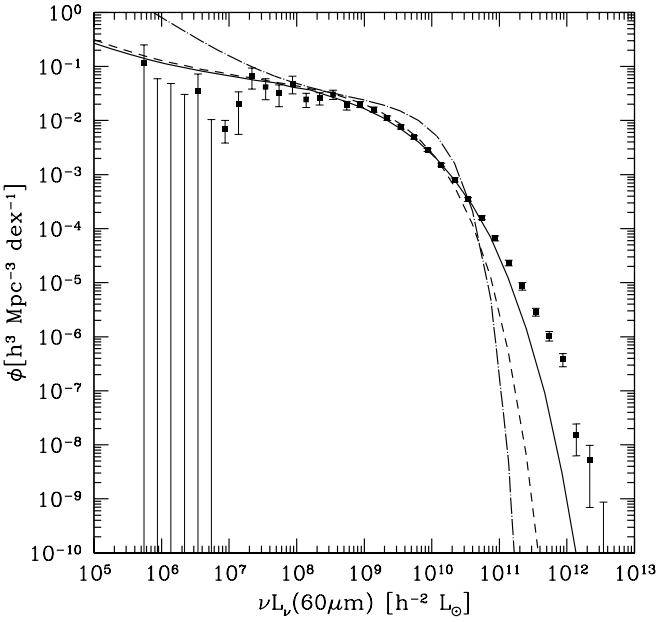

FIG. 6.— Infrared luminosity function of galaxies at 60μm. The data are taken from Saunders et al. (1990). The solid and dashed lines are the prediction of our model assuming the screen and slab distribution of dust, respectively. Considering the uncertainty in the normalization of luminosity function, the normalization of model curves are set to match the data in the range of $\nu L_\nu(60\mu\mathrm{m}) \leq 10^{11}h^{-2}L_\odot$. [More luminous galaxies are removed from normalization fit to avoid contamination of AGNs which is expected to be significant for ultraluminous galaxies (Veilleux, Kim, & Sanders 1999).] The dot-dashed line is the prediction from the Schechter-type *B*-band luminosity function when the infrared luminosity is simply proportional to the *B*-band luminosity in all galaxies as $\nu L_\nu(B)/\nu L_\nu(60\mu\mathrm{m})$=1.

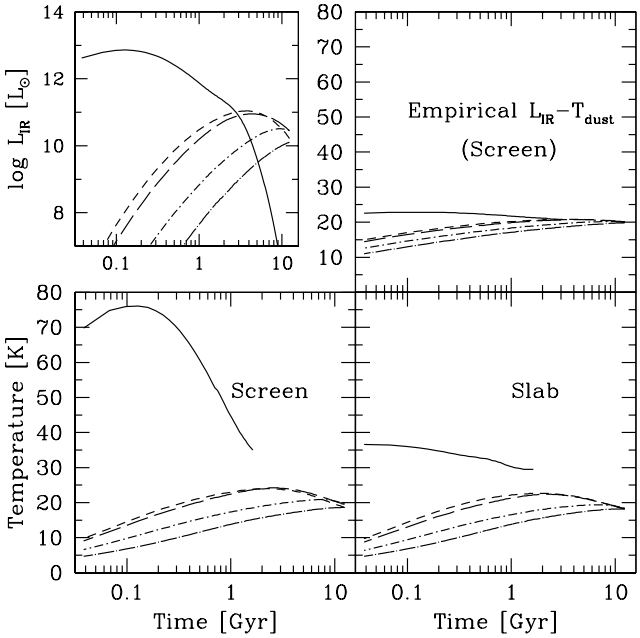

FIG. 7.— The evolution of infrared luminosity and characteristic temperature of big grain dust predicted by our model as a function of time after the formation, for five types of galaxies: E/S0 (solid), Sab (short-dashed), Sbc (long-dashed), Scd (dot-short-dashed), and Sdm (dot-long-dashed). The upper-left panel shows the evolution of total infrared luminosity of our model assuming the screen-type dust. The upper-right panel shows the temperature evolution predicted when one uses the empirical $L_{\rm IR}$-$T_{\rm dust}$ relation observed for local infrared galaxies. The lower-left and -right panels show the predictions of dust temperature evolution based on our model taking into account the energy balance between absorption and re-emission of stellar light, for the screen- and slab-type dust distributions, respectively. All models are for galaxies whose luminosity is M_B = –20 at z = 0.

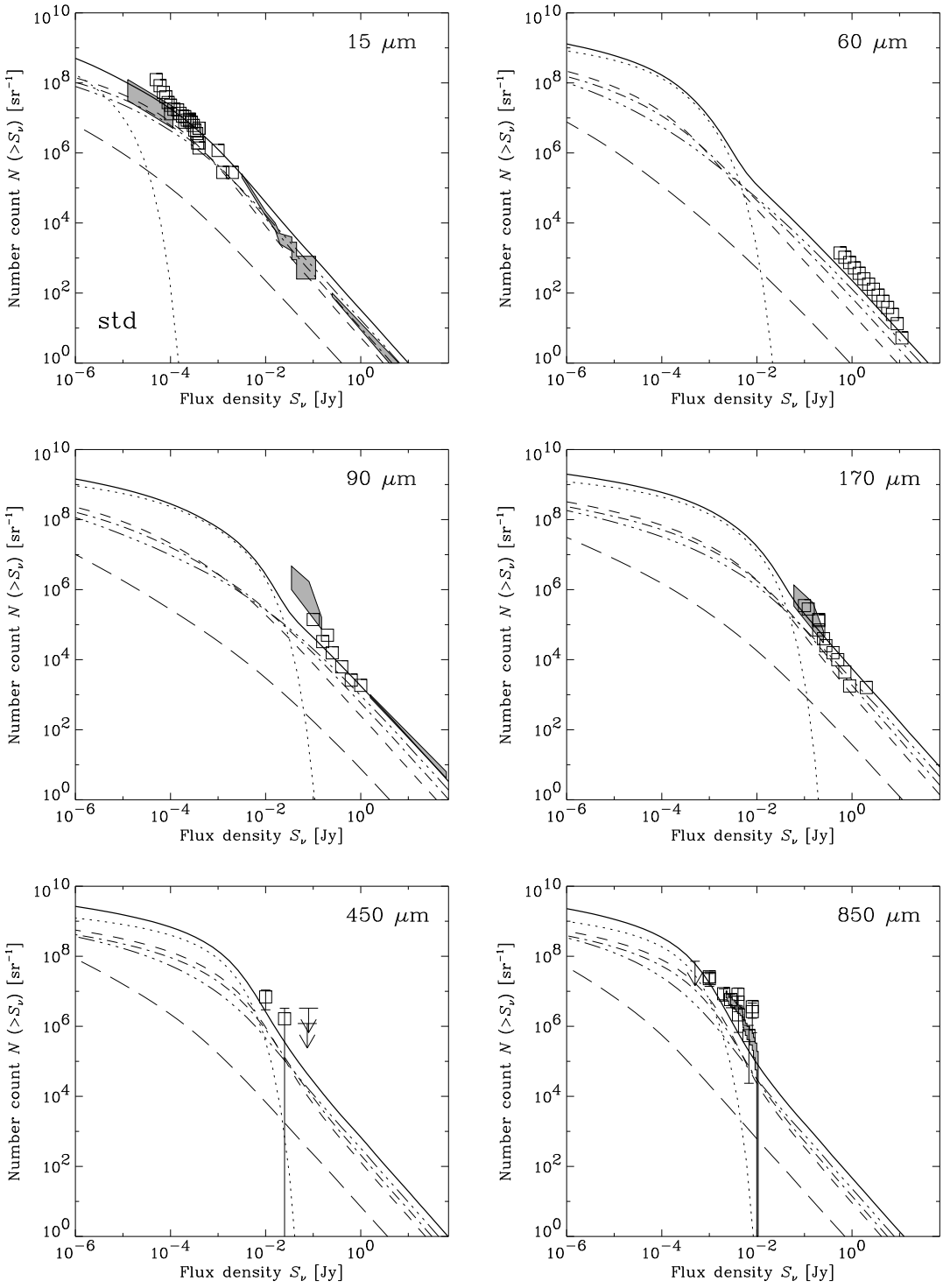

FIG. 8.— Faint galaxy counts in infrared and submillimeter bands. The solid line is the prediction by our baseline model with a cosmological model of $(h, \Omega_0, \Omega_\Lambda) = (0.7, 0.2, 0.8)$, pure luminosity evolution, formation redshift of $z_F = 3$, and screen-type distribution of dust. The solid line is the total of all galaxy types, while the other five lines are for individual types: E/S0 (dotted), Sab (short-dashed), Sbc (dot-dashed), Scd (three-dot-dashed) and Sdm (long-dashed). The data are taken from the following references: Rush et al. (1993), Oliver et al. (1997), Flores et al. (1999a, b), Clements et al. (1999), Aussel et al. (1999), Altieri et al. (1999), Elbaz et al. (1999), and Serjeant et al. (2000) (15 μm); Rowan-Robinson et al. (1991) (60 μm); Juvela et al. (2000), Matsuhara et al. (2000), Efstathiou et al. (2000), and *IRAS* 100 μm galaxy counts (90 μm); Stickel et al. (1998), Kawara et al. (1998), Puget et al. (1999), Juvela et al. (2000), Matsuhara et al. (2000), and Dole et al. (2001) (170 μm); Smail et al. (1997), Barger, Cowie, & Sanders (1999), and Blain et al. (2000) (450 μm); and Smail, Ivison, & Blain (1997), Hughes et al. (1998), Blain et al. (1999), Eales et al. (1999, 2000), Holland et al. (1999), and Barger et al. (1998, 1999) (850 μm).

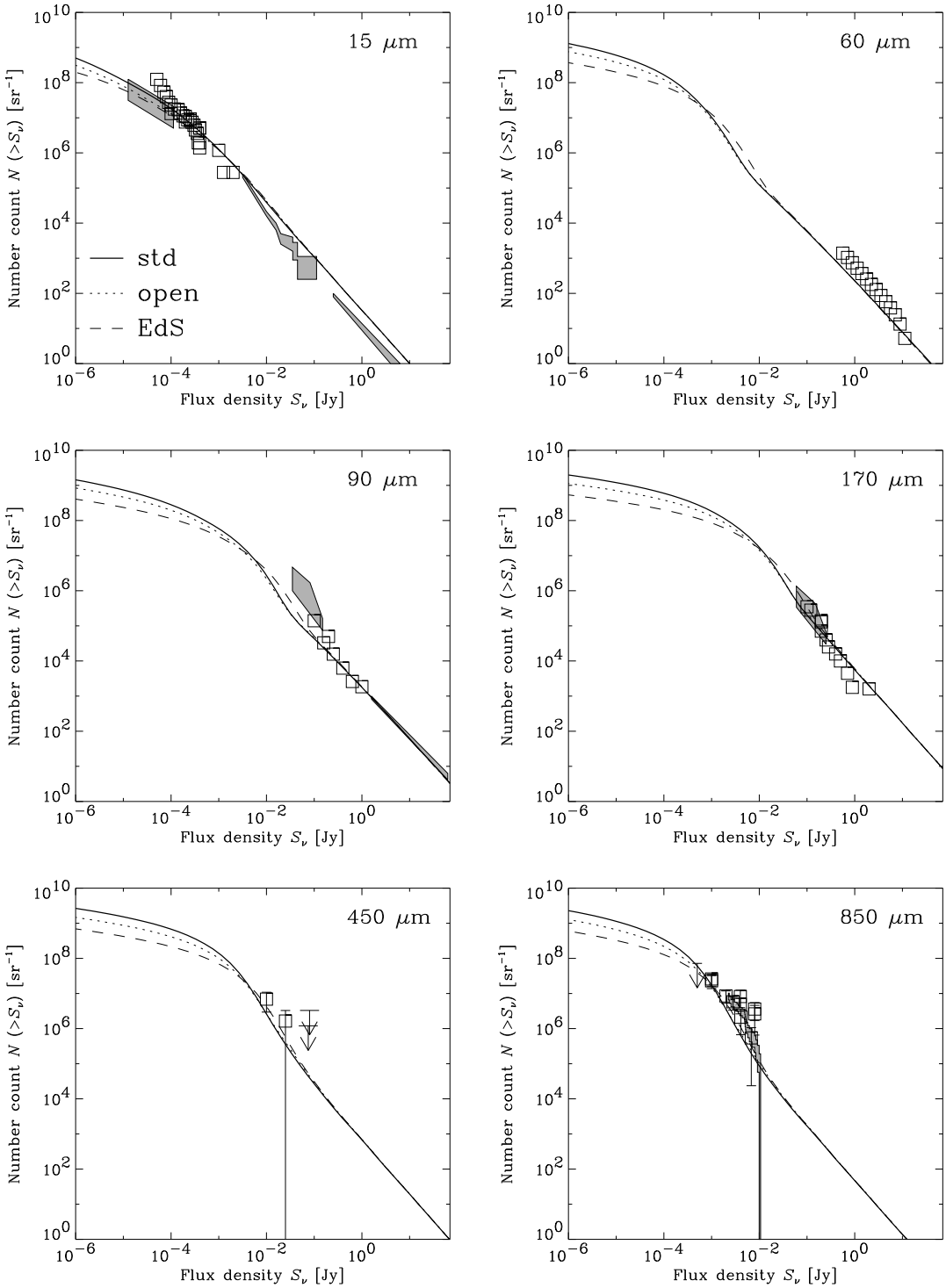

FIG. 9.— The same as Fig. 8, but for different cosmological models: the Λ-dominated flat universe with $(h, \Omega_0, \Omega_\Lambda)$ = (0.7, 0.2, 0.8) (solid, the baseline model shown in Fig. 8), an open universe with (0.7, 0.2, 0.0) (dotted), and an Einstein-de Sitter universe with (0.5, 1, 0) (dashed).

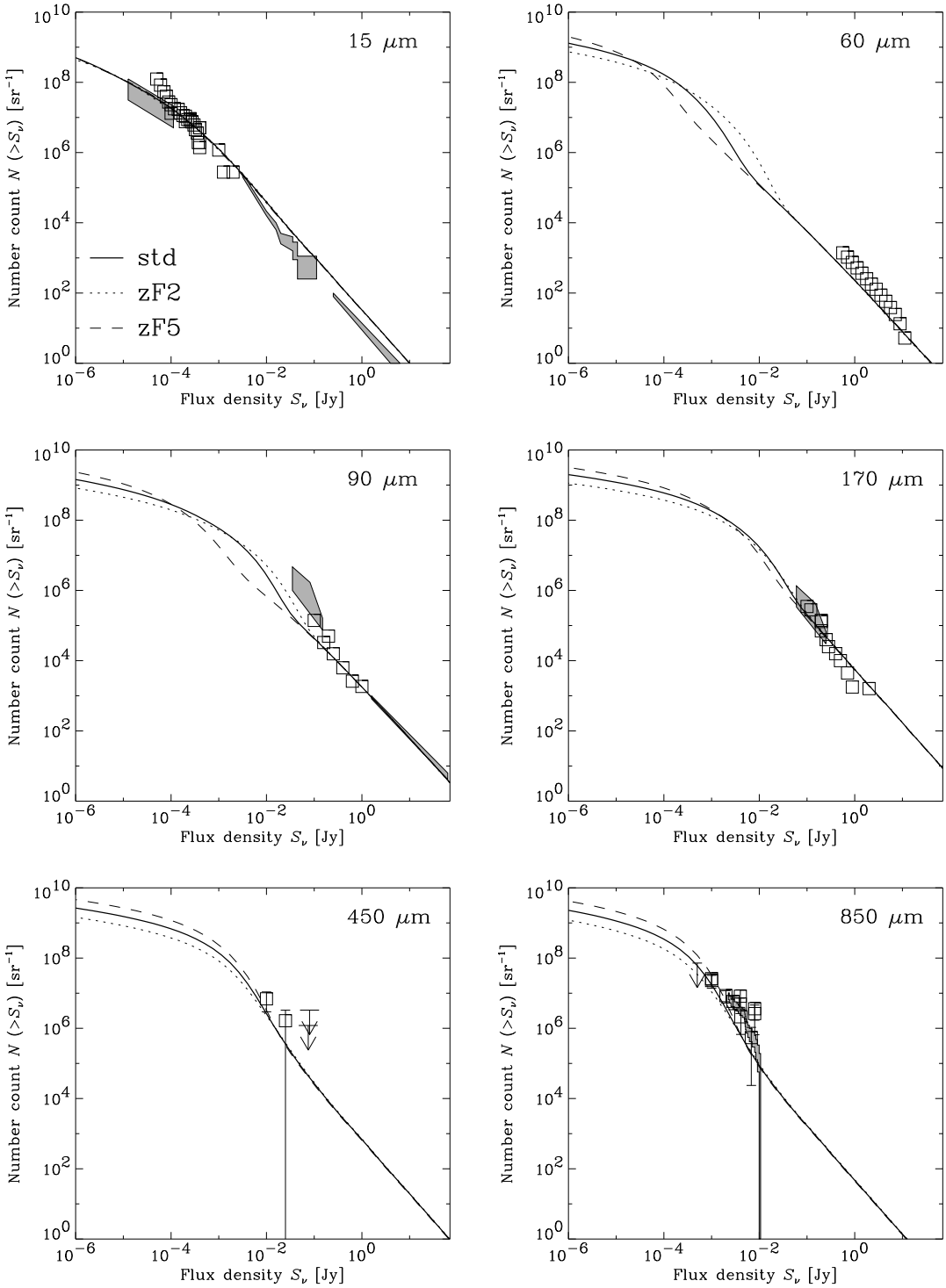

FIG. 10.— The same as Fig. 8, but for different formation redshift of galaxies: z_F = 2 (dotted), z_F = 3 (solid, the baseline model shown in Fig. 8), and z_F = 5 (dashed).

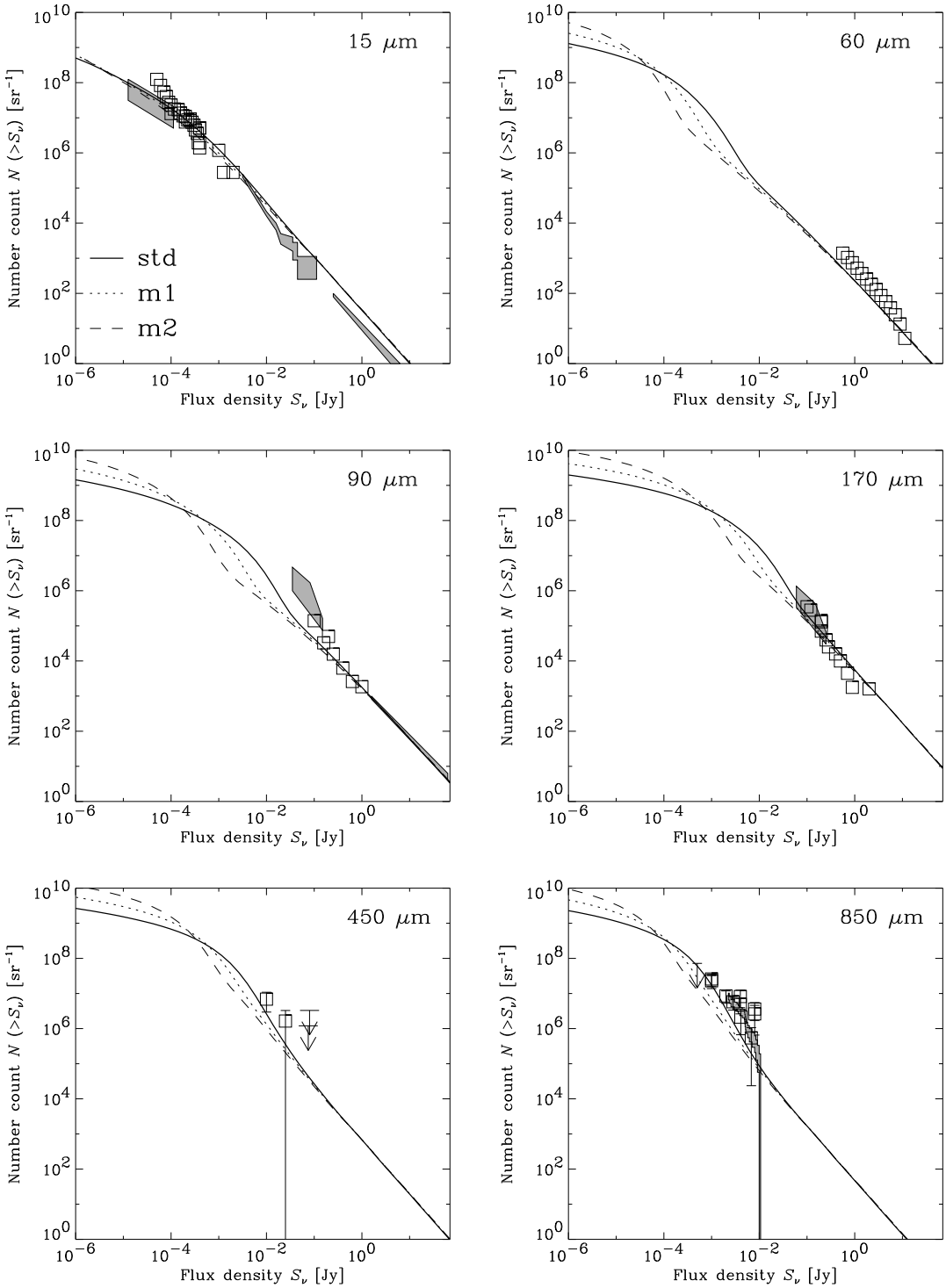

FIG. 11.— The same as Fig. 8, but for the cases of number evolution of galaxies: $\eta = 0$ (solid, the baseline model without number evolution shown in Fig. 8), $\eta = 1$ (dotted), and $\eta = 2$ (dashed). See text for the modeling of number evolution.

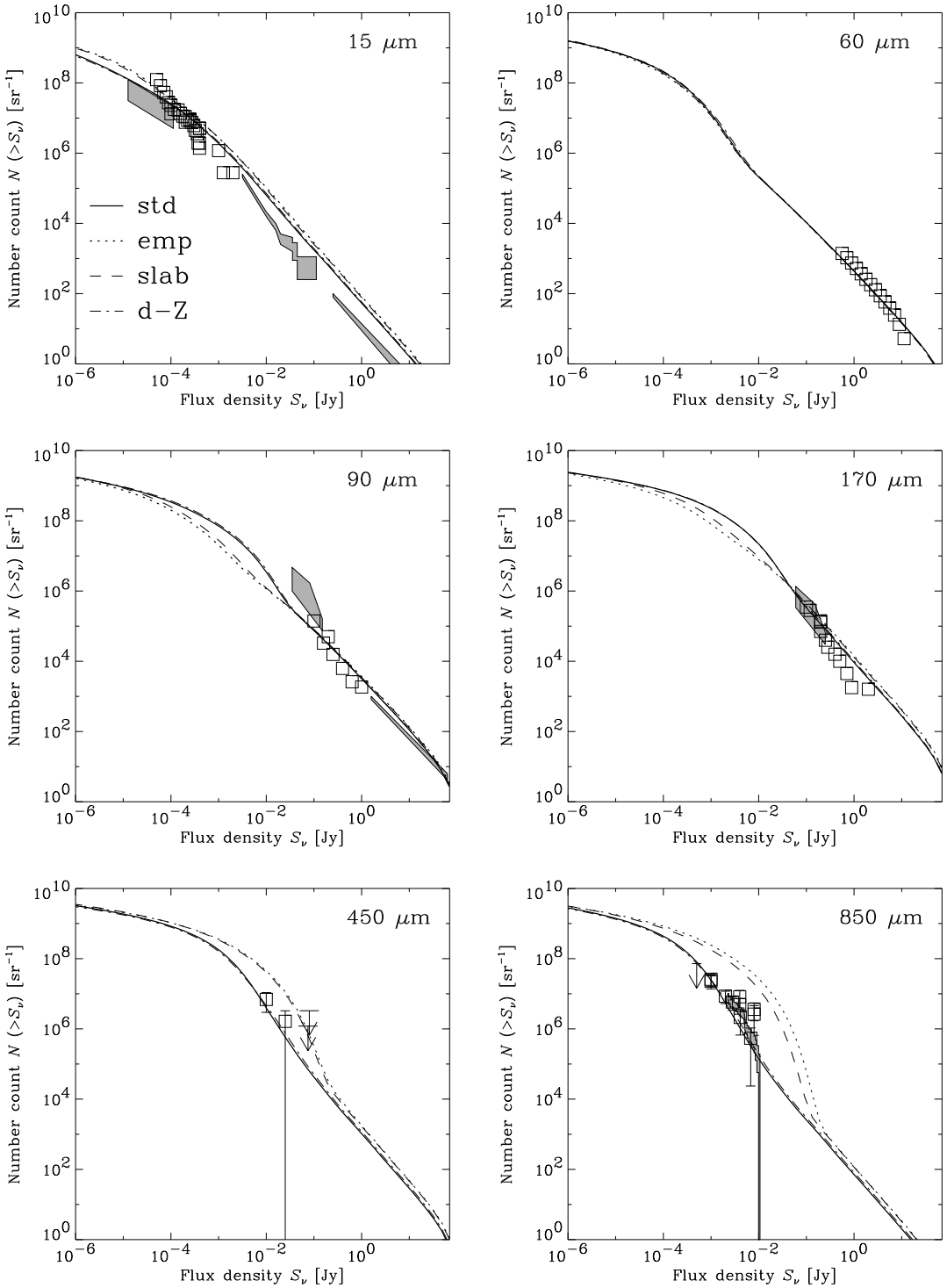

FIG. 12.— The same as Fig. 8, but with different model prescriptions from the baseline model (solid line, and shown in Fig.8): empirical $L_{\rm IR}$-$T_{\rm dust}$ relation (dotted), slab-type dust (dashed), and non-proportional dust/metal ratio (dot-dashed).

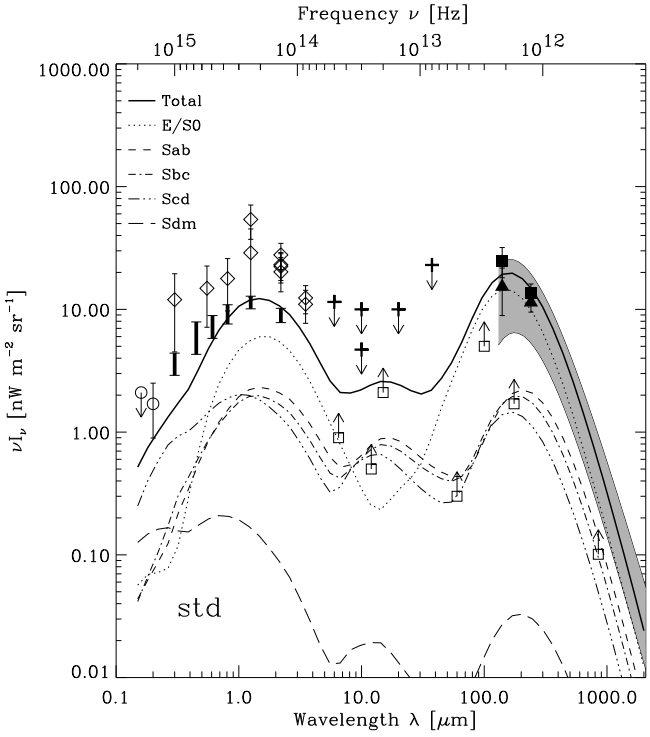

FIG. 13.— Spectrum of the cosmic background radiation (CBR) from optical to FIR bands. The solid line is the prediction by our baseline model, and the other five lines show the contribution from individual types of galaxies, as indicated in the figure. References for the observational data are as follows; UV data shown by open circles: Martin, Hurwitz, & Bowyer (1991; 1600 Å) and Armand et al. (1994; 2000 Å). Ranges estimated from integration of optical/NIR galaxy counts: Totani et al. (2001a, thick error bars without symbols). Reports for diffuse CBR detections at optical and NIR bands are shown by open diamonds: Bernstein, Freedman, & Madore (2002; 0.3, 0.55, and 0.8μm), Gorjian et al. (2000; 2.2 and 3.5μm), Wright & Reese (2000; 2.2 and 3.5μm), Cambrésy et al. (2001; 1.25 and 2.2μm), and Wright (2001; 1.25 and 2.2μm). Lower limits from infrared/submillimeter galaxy count integrations shown by open squares: Gispert et al. (2000; 6.5 μm), Clements et al. (1999; 12 μm), Elbaz et al. (1999; 15 μm), Lonsdale et al. (1990; 60 μm), Dwek et al. (1998; 90 μm), Puget et al. (1999; 175 μm), Barger et al. (1999; 850 μm). MIR upper limits from TeV gamma-ray observations shown by thick crosses: Biller et al. (1998) and Renault et al. (2001). *COBE*/DIRBE detections at 140 and 240 μm: Hauser et al. (1998, filled squares) and Lagache et al. (2000, filled triangles). *COBE*/FIRAS detection at 100 μm – 1 mm shown by the shaded area: Fixsen et al. (1998).

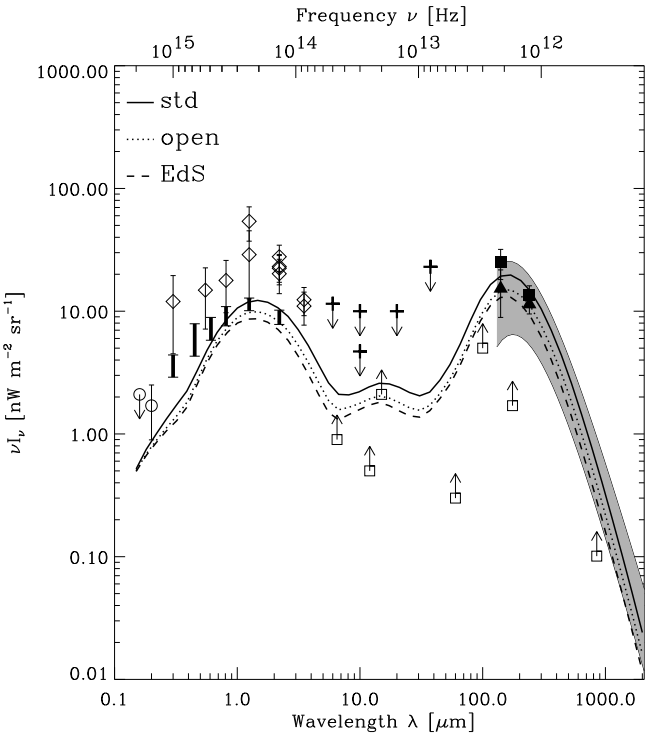

FIG. 14.— The same as Fig. 13, but for different cosmological models: the Λ-dominated flat universe with $(h, \Omega_0, \Omega_\Lambda) = (0.7, 0.2, 0.8)$ (solid, the baseline model shown in Fig. 13), an open universe with (0.7, 0.2, 0.0) (dotted), and an Einstein-de Sitter universe with (0.5, 1, 0) (dashed).

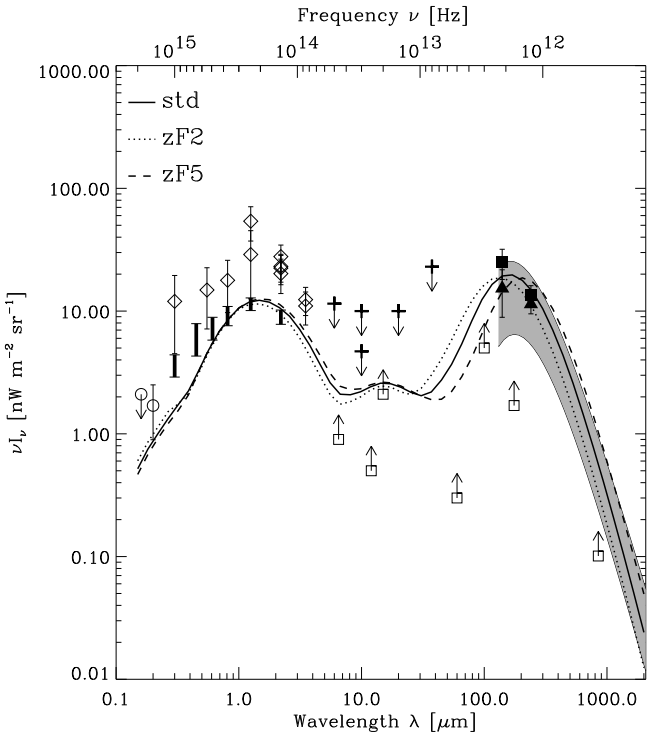

FIG. 15.— The same as Fig. 13, but for different formation redshift of galaxies: z_F = 2 (dotted), z_F = 3 (solid, the baseline model shown in Fig. 13), and z_F = 5 (dashed).

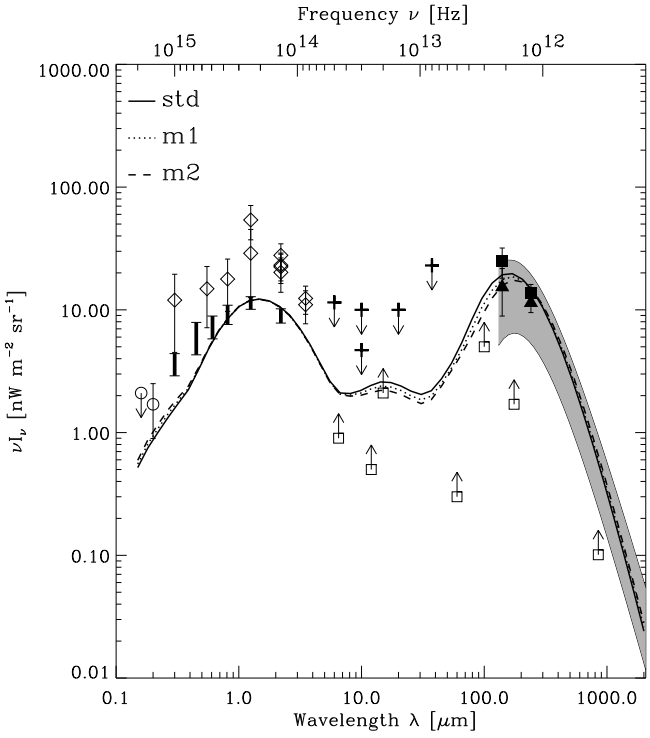

FIG. 16.— The same as Fig. 13, but for the cases of number evolution of galaxies: η = 0 (solid, the baseline model without number evolution shown in Fig. 13), η = 1 (dotted), and η = 2 (dashed). See text for the modeling of number evolution.

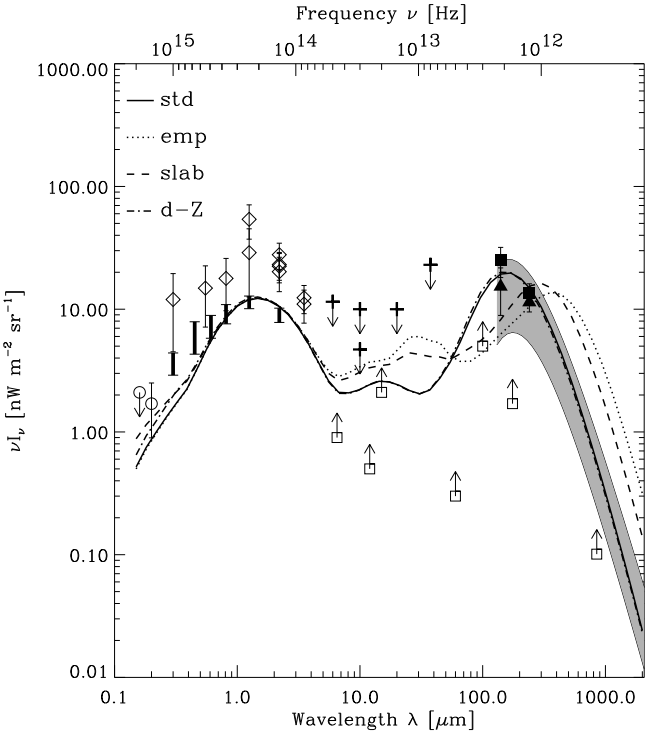

FIG. 17.— The same as Fig. 13, but with different model prescriptions from the baseline model (solid line, and shown in Fig.13): empirical $L_{\rm IR}$-$T_{\rm dust}$ relation (dotted), slab-type dust (dashed), and non-proportional dust/metal ratio (dot-dashed).

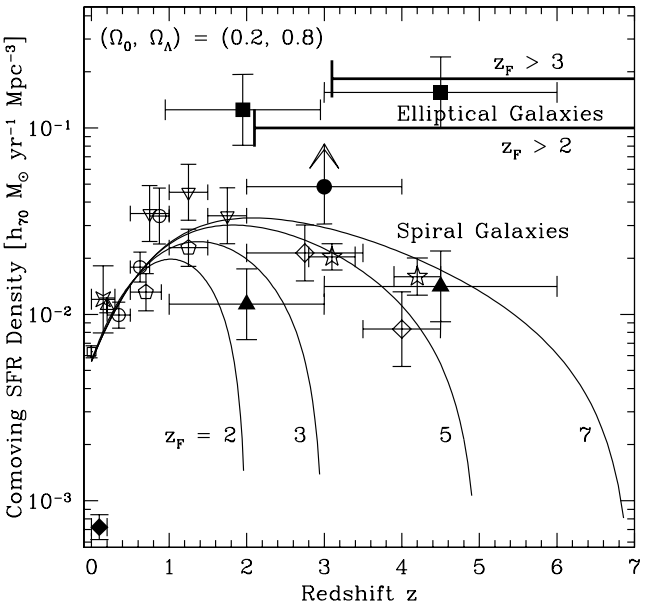

FIG. 18.— Cosmic history of global star formation rate. The solid curves are the prediction of our baseline model for spiral galaxies (i.e., except for elliptical galaxies), with several values of z_F. The two horizontal solid lines are mean SFR of elliptical galaxies when they are assumed to be formed before z_F= 2 or 3, respectively. The observed data for dust-uncorrected SFR from Hα or UV luminosity density (i.e., unabsorbed SFR) are shown by open symbols: Gallego et al. (1995, square), Tresse & Maddox (1998, triangle), Treyer et al. (1998. four-edged star), Lilly et al. (1996, open circles), Connolly et al. (1997, upside-down triangles), Madau, Pozzetti, & Dickinson (1998, diamonds), Steidel et al. (1999, five-edged stars), Cowie, Songaila, & Barger (1999, pentagons). The SFR density inferred from submillimeter observations (i.e., hidden SFR) are shown by filled symbols: Hughes et al. (1998, circle); Barger, et al. (2000) before (triangles) and after (squares) the completeness corrections. The local hidden SFR density from ULIRGs is shown by the filled diamond (Barger et al. 2000). These observed data have been corrected for the cosmological parameters chosen here $[(h, \Omega_0, \Omega_\Lambda) = (0.7, 0.2, 0.8)]$.

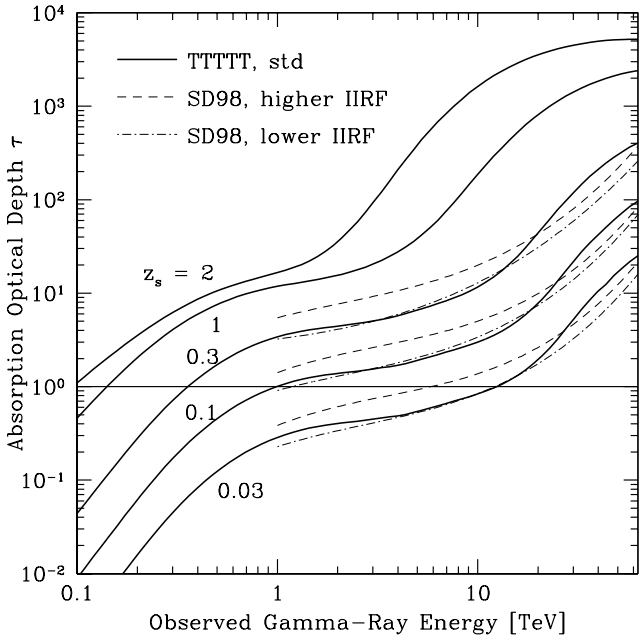

FIG. 19.— The intergalactic optical depth of very high energy gamma-rays to the absorption by interaction with optical/infrared cosmic background radiation, as a function of the source redshift (z_s) and the gamma-ray energy observed at z = 0. The solid lines are the calculation based on our baseline model, with the source redshifts indicated in the figure (indicated as TTTTT from the initials of the authors). For comparison, calculations with 'higher IIRF SED' (dashed line) and 'lower IIRF SED' (dot-dashed line) by Stecker & de Jager (1998) are plotted for z_s = 0.03, 0.1, and 0.3 (from the bottom to the top).